



HAL
open science

Variance based sensitivity analysis for Monte Carlo and importance sampling reliability assessment with Gaussian processes

Morgane Menz, Sylvain Dubreuil, Jérôme Morio, Christian Gogu, Nathalie Bartoli, Marie Chiron

► **To cite this version:**

Morgane Menz, Sylvain Dubreuil, Jérôme Morio, Christian Gogu, Nathalie Bartoli, et al.. Variance based sensitivity analysis for Monte Carlo and importance sampling reliability assessment with Gaussian processes. *Structural Safety*, 2021, 93, pp.102116. 10.1016/j.strusafe.2021.102116. hal-03324347

HAL Id: hal-03324347

<https://ut3-toulouseinp.hal.science/hal-03324347>

Submitted on 23 Aug 2021

HAL is a multi-disciplinary open access archive for the deposit and dissemination of scientific research documents, whether they are published or not. The documents may come from teaching and research institutions in France or abroad, or from public or private research centers.

L'archive ouverte pluridisciplinaire **HAL**, est destinée au dépôt et à la diffusion de documents scientifiques de niveau recherche, publiés ou non, émanant des établissements d'enseignement et de recherche français ou étrangers, des laboratoires publics ou privés.

Variance based sensitivity analysis for Monte Carlo and importance sampling reliability assessment with Gaussian processes

Morgane Menz^{a,b}, Sylvain Dubreuil^b, Jérôme Morio^b, Christian Gogu^a,
Nathalie Bartoli^b, Marie Chiron^b

^a *Université de Toulouse, UPS, CNRS, INSA, Mines Albi, ISAE, Institut Clément Ader (ICA), 3 rue Caroline Aigle, 31400 Toulouse, France*

^b *ONERA/DTIS, Université de Toulouse, F-31055 Toulouse, France*

Abstract

Running a reliability analysis on engineering problems involving complex numerical models can be computationally very expensive, requiring advanced simulation methods to reduce the overall numerical cost. Gaussian process based active learning methods for reliability analysis have emerged as a promising way for reducing this computational cost. In this paper, we propose a methodology to quantify the sensitivity of the failure probability estimator to uncertainties generated by the Gaussian process and the sampling strategy. This quantification also enables to control the whole error associated to the failure probability estimate and thus provides an accuracy criterion on the estimation. Thus, an active learning approach integrating this analysis to reduce the main source of error and stopping when the global variability is sufficiently low is introduced. The approach is proposed for both a Monte Carlo based method as well as an importance sampling based method, seeking to improve the estimation of rare event probabilities. Performance of the proposed strategy is then assessed on several examples.

Keywords: Failure probability, Reliability, Monte Carlo, Importance Sampling, Active learning, Gaussian process, Sensitivity analysis, Classification

1. Introduction

Engineering systems are subject to numerous uncertainties that imply a probability that these systems can fail. Reliability analyses seek to determine this probability of failure in order to understand, certify or improve their design. Numerous reliability analysis techniques, i.e. techniques to estimate the probability of failure, can be found in the literature such as analytic approximations (FORM/SORM) [1], sampling methods based on Monte Carlo Simulations techniques [2], surrogate-based reliability analysis methods [3], which can be adaptive or not. Adaptive approaches have been proposed in particular for Gaussian process surrogates [4, 5, 6, 7, 8, 9, 10, 11], support vector machines [12, 13] and polynomial-chaos-based Kriging [14]. Considering any sampling technique, the probability of failure is obtained by a classification of the samples. The latter have to be evaluated first in order to be classified. This evaluation phase can be numerically very expensive for complex models. Gaussian process-based adaptive sampling methods for reliability analysis represent one of the promising ways for reducing this computational cost.

Gaussian process-based adaptive sampling methods consist in building a Gaussian process surrogate model (or Kriging surrogate model) [15, 16] of the performance function and using the uncertainty structure of the Gaussian process to enrich iteratively this surrogate model. For that purpose, a learning criterion is used to select enrichment points at each iteration of the learning phase in order to better learn the limit state. Then, the estimation of the probability of failure is typically obtained by a classification of a set of Monte Carlo samples evaluated on the final surrogate model.

Several adaptive methods have been proposed along these lines, such as the efficient global reliability analysis (EGRA) by Bichon et. al [6] or Active learning reliability method combining Kriging and Monte Carlo Simulations (AK-MCS) by Echard et. al [17]. Other methods have also been presented to address specific problems such as small failure probabilities (rare events) estimations [5, 18, 19, 20, 11, 9, 21], multiple failure regions problems [22, 23, 24, 25] or systems

failure probabilities assessment [8, 26, 7, 4, 10, 27].

In adaptive surrogate based methods, the estimator of the probability of failure is affected by two different uncertainty sources related to the surrogate model approximation and to the Monte Carlo (MC) based integration technique. Some investigations have already been carried out to take into account the Gaussian process accuracy on the quantity of interest (failure probability estimator), instead of the Gaussian process local error in the vicinity of the limit state. In [14] some bounds of the estimator or in [28] an approximation of the estimation relative error are used. None of these works have however thought to specifically separate the two previously described sources of error.

In this paper, we propose to analyse both the Monte Carlo sampling and the surrogate model influence on the probability of failure estimator with variance based sensitivity indexes. We show that it is possible to estimate them numerically. It enables us to analyse quantitatively the source of uncertainty that has to be reduced to improve the accuracy of the failure probability estimate. We finally propose a new reliability assessment algorithm that integrates this analysis to focus on the main source of uncertainty during the learning phase and also provides a stopping criterion based on the whole error associated to the failure probability estimate.

The rest of the paper is organized as following. First, we present estimators of the sensitivity indices of the probability of failure and also of the total variance. Then, we propose a reliability analysis algorithm that integrates this sensitivity analysis to adaptively improve the major source of uncertainty during the learning phase. A stopping criterion based on the total variance estimation is also proposed for this algorithm. Finally, we present an extension of the method adapted to tackle rare events probability estimation problems.

2. Reliability analysis

2.1. General setting of reliability analyses

Let x_1, \dots, x_m be the m uncertain parameters that are input to the reliability
60 problem. These parameters are modeled by an absolutely continuous random
vector \mathbf{X} of random variables X^k , $k = 1, \dots, m$ characterized by a joint proba-
bility distribution with probability density function $f_{\mathbf{X}}$. Note that the random
vector \mathbf{X} could be either in the physical or in the standard normal space. In
the rest of the paper we will consider it in the physical space.

In the context of reliability, the output of interest is the performance function
 $G : \mathbb{R}^m \rightarrow \mathbb{R}$. This function characterizes the failure of a system. Hence the
domain of failure reads $\mathcal{D}_f = \{\mathbf{x} \in \mathbb{R}^m, G(\mathbf{x}) \leq 0\}$, the domain of safety reads
 $\{\mathbf{x} \in \mathbb{R}^m, G(\mathbf{x}) > 0\}$ and the limit state is $\{\mathbf{x} \in \mathbb{R}^m, G(\mathbf{x}) = 0\}$. The failure
probability P_f is then defined as:

$$P_f = \mathbb{E}_{f_{\mathbf{X}}} [\mathbb{1}_{G(\mathbf{X}) \leq 0}] = \int_{\mathbb{R}^m} \mathbb{1}_{G(\mathbf{x}) \leq 0} f_{\mathbf{X}}(\mathbf{x}) d\mathbf{x} \quad (1)$$

65 where $\mathbb{1}_{G(\mathbf{x}) \leq 0}$ is an indicator function. Several methods exist to evaluate
this probability [29]. One of the simplest methods is Monte Carlo Simula-
tion (MCS). It consists in the generation of n_{MC} random independent and
identically distributed (i.i.d) samples $\mathbf{X}_1, \dots, \mathbf{X}_{n_{MC}}$ with distribution $f_{\mathbf{X}}$ and
computing an estimation of the failure probability using these samples. As the
70 failure probability can be expressed as a mathematical expectation (see Eq. (1)),
the law of large numbers suggests to build its estimator as the empirical mean
of $(\mathbb{1}_{G(\mathbf{X}_i) \leq 0})_{i=1, \dots, n_{MC}}$.

An estimation \hat{P}_f^{MC} of the failure probability P_f is then given by:

$$\hat{P}_f^{MC} = \frac{1}{n_{MC}} \sum_{i=1}^{n_{MC}} \mathbb{1}_{G(\mathbf{x}) \leq 0}(\mathbf{X}_i) \quad (2)$$

The variance of this estimator is defined by:

$$Var(\hat{P}_f^{MC}) = \frac{Var(\mathbb{1}_{G(\mathbf{X}_1) \leq 0}(\mathbf{X}_1))}{n_{MC}} \quad (3)$$

Hence, MCS based classification methods need a lot of simulations to estimate small failure probabilities. In order to avoid the evaluation of a complex performance function $G(\mathbf{x})$ on a whole Monte Carlo population, an approximation
75 by a surrogate model, denoted $\hat{G}(\mathbf{x})$, of this function can be used instead.

2.2. Reliability analysis using a Gaussian process

Reliability analysis with a surrogate model relies mainly on four elements:

- the type of surrogate model. Throughout the article, the surrogate model
80 $\hat{G}(\mathbf{x})$ is assumed to be a Gaussian process and we will review its basics in Sec. 2.2.1.
- the sampling approach. In this article, we only consider Monte Carlo based sampling approaches such as MCS or importance sampling (see Sec. 2.1 and Sec. 5.1).
- 85 • the surrogate model enrichment criterion used to most appropriately enrich the surrogate model in order to achieve an accurate approximation of the limit state. (see Sec. 2.2.2)
- the algorithm stopping criterion, that is set to determine when the surrogate model learning is sufficient to obtain an accurate classification of the
90 samples. (see Sec. 2.2.2)

In the introduction, many Gaussian process active learning methods were mentioned. Here, we are interested in methods that consider a population of candidate samples for the learning. This strategy has been first proposed in the AK-MCS [17] method. Other methods have then been proposed in order to
95 address more complex reliability problems as discussed in the introduction. In Sec. 2.2.2, some enrichment criteria and their corresponding stopping criteria used in these methods will be analyzed.

2.2.1. *The Gaussian Process surrogate model*

Gaussian process regression, introduced in geostatistics by Krige [30] and
 100 formalized later by Matheron [31], is a method of interpolation in which the
 interpolated function is modeled by a Gaussian process.

A Kriging or Gaussian process interpolation (GP) [15], denoted by \mathcal{G} , is fully
 characterized by its mean function $m(\mathbf{x})$ and a kernel (or covariance function)
 $k(\cdot, \cdot)$. Hence, the GP prior can be defined as:

$$\mathcal{G}(\mathbf{x}) = m(\mathbf{x}) + Z(\mathbf{x}) \tag{4}$$

where:

- $m(\mathbf{x}) = \mathbf{f}(\mathbf{x})^T \boldsymbol{\beta}$ with $\mathbf{f}(\mathbf{x})$ a vector of basis functions and $\boldsymbol{\beta}$ the associated regression coefficients.
- $Z(\mathbf{x})$ a stationary, zero mean, Gaussian process with the variance σ_Z^2 such that the kernel defining the GP is

$$k(\mathbf{x}, \mathbf{x}') = \text{CoVar}(\mathcal{G}(\mathbf{x}), \mathcal{G}(\mathbf{x}')) = \sigma_Z^2 r_\theta(\mathbf{x}, \mathbf{x}')$$

105 $r_\theta(\mathbf{x}, \mathbf{x}')$ being a correlation function defined by the hyperparameter set
 $\boldsymbol{\theta}$ and $\text{CoVar}(\cdot, \cdot)$ being the covariance function between two points. In
 this paper, only stationary kernels are used, which means that kernels are
 functions of $\mathbf{d} = |\mathbf{x} - \mathbf{x}'|$ (i.e. $r_\theta(\mathbf{x}, \mathbf{x}') = r_\theta(\mathbf{d})$).

Several kernel models are available to define the correlation function, such
 110 as the squared exponential, Matern $3/2$ or Matern $5/2$, the latter one being used
 in the rest of the paper.

The hyperparameters $\boldsymbol{\theta}$, σ_Z and $\boldsymbol{\beta}$ of the GP must be estimated to approxi-
 mate the response for any unknown point of the domain. For a fixed kernel type,
 several techniques exist to obtain the optimal values of these hyperparameters,
 115 for example by Maximum Likelihood Estimation [32] or cross-validation [15].

The prior distribution of \mathcal{G} is considered to be Gaussian. Hence, the pos-
 terior distribution \mathcal{G}_n of \mathcal{G} knowing the observations $\{\mathbf{x}_{doe} = (\mathbf{x}_1, \dots, \mathbf{x}_n), \mathbf{y} =$

$G(\mathbf{x}_{doe})\}$ is Gaussian $\mathcal{G}_n = \mathcal{G}(\mathbf{x}_{doe}, y) \sim GP(\mu_n(\cdot), \sigma_n^2(\cdot, \cdot))$. The GP predictor $\hat{G}(\mathbf{x})$ associated to the response has its mean value $\mu_n(\mathbf{x})$ and covariance $\sigma_n^2(\mathbf{x}, \mathbf{x}')$ given by:

$$\mu_n(\mathbf{x}) = \mathbf{f}(\mathbf{x})^T \hat{\boldsymbol{\beta}} + \mathbf{k}(\mathbf{x})^T \mathbf{C}^{-1} (\mathbf{y} - \mathbf{F} \hat{\boldsymbol{\beta}}) \quad (5)$$

$$\sigma_n^2(\mathbf{x}, \mathbf{x}') = \mathbf{k}(\mathbf{x}, \mathbf{x}') - \begin{pmatrix} \mathbf{k}(\mathbf{x})^T & \mathbf{f}(\mathbf{x})^T \end{pmatrix} \begin{pmatrix} \mathbf{C} & \mathbf{F}^T \\ \mathbf{F} & \mathbf{0} \end{pmatrix}^{-1} \begin{pmatrix} \mathbf{k}(\mathbf{x}') \\ \mathbf{f}(\mathbf{x}') \end{pmatrix} \quad (6)$$

where $\mathbf{k}(\mathbf{x}) = (k(\mathbf{x}, \mathbf{x}_1), \dots, k(\mathbf{x}, \mathbf{x}_n))^T$, \mathbf{F} is the matrix with row i equals to $\mathbf{f}(\mathbf{x}_i)^T$, $\mathbf{C} := (k(\mathbf{x}_i, \mathbf{x}_j))_{i,j}$ is the covariance matrix between the observations, and $\hat{\boldsymbol{\beta}} = (\mathbf{F}^T \mathbf{C}^{-1} \mathbf{F})^{-1} \mathbf{F}^T \mathbf{C}^{-1} \mathbf{y}$.

Note that in the rest of the paper we will assume that $m(\mathbf{x})$ is an unknown
 120 constant to be fitted with the other hyperparameters (also known as ordinary Kriging assumption).

In the following section, the principle of adaptive sampling reliability analysis methods based on an active learning of a Gaussian process will be presented.

2.2.2. Gaussian process based reliability methods

125 Gaussian process based reliability methods consist in the learning of a GP of the performance function $G(\mathbf{x})$. Therefore, the Gaussian process is iteratively enriched throughout a learning process in order to be sufficiently accurate in the vicinity of the limit state. The constructed surrogate model is thus well-suited for the classification of samples and allows to obtain an accurate estimation of
 130 the probability of failure.

The selection of the best enrichment point, with respect to the improvement of the GP approximation of the limit state, among all candidate samples, is based on a specific learning criterion. These learning criteria are built based on learning functions used to determine the most relevant point to evaluate the performance function at each iteration of the algorithm. Many learning functions exist but we will focus here on two classic learning functions that are

the functions U and EFF . The function U proposed in [17] is given by:

$$U(\mathbf{x}) = \frac{|\mu_n(\mathbf{x})|}{\sigma_n(\mathbf{x})} \quad (7)$$

This criterion is evaluated on the Monte Carlo population and the next enrichment point is selected as the sample \mathbf{x} that minimizes U . In AK-MCS [17], the learning stopping condition for U is defined as $\min_{\mathbf{x}}(U(\mathbf{x})) \geq 2$.

Another learning criterion is the expected feasibility function $EFF(\mathbf{x})$, initially coming from the EGRA method [6], and is given by the following expression:

$$\begin{aligned} EFF(\mathbf{x}) = & \mu_n(\mathbf{x}) \left[2\Phi\left(-\frac{\mu_n(\mathbf{x})}{\sigma_n(\mathbf{x})}\right) - \Phi\left(-\frac{\epsilon + \mu_n(\mathbf{x})}{\sigma_n(\mathbf{x})}\right) - \Phi\left(\frac{\epsilon - \mu_n(\mathbf{x})}{\sigma_n(\mathbf{x})}\right) \right] \\ & - \sigma_n(\mathbf{x}) \left[2\phi\left(-\frac{\mu_n(\mathbf{x})}{\sigma_n(\mathbf{x})}\right) - \phi\left(-\frac{\epsilon + \mu_n(\mathbf{x})}{\sigma_n(\mathbf{x})}\right) - \phi\left(\frac{\epsilon - \mu_n(\mathbf{x})}{\sigma_n(\mathbf{x})}\right) \right] \\ & + \epsilon \left[\Phi\left(\frac{\epsilon - \mu_n(\mathbf{x})}{\sigma_n(\mathbf{x})}\right) - \Phi\left(-\frac{\epsilon + \mu_n(\mathbf{x})}{\sigma_n(\mathbf{x})}\right) \right] \end{aligned} \quad (8)$$

where $\Phi(\cdot)$ is the standard normal cumulative distribution function and $\phi(\cdot)$ the standard normal density function. In EGRA and AK-MCS+ EFF , the expected feasibility function is built with $\epsilon = 2\sigma_n$. At each iteration, the next best point to evaluate is then the candidate sample whose EFF value is maximum. The learning stopping condition is based on a stopping value of the learning criterion and is defined as:

$$\max_{\mathbf{x}}(EFF(\mathbf{x})) \leq 0.001$$

The probability of failure estimation on a Monte Carlo population of n_{MC} samples $\tilde{\mathbf{X}} = (\mathbf{X}_i)_{i=1, \dots, n_{MC}}$ with \mathbf{X}_i i.i.d. with the same probability distribution as \mathbf{X} is then given by:

$$\hat{P}_f^{MC}(\tilde{\mathbf{X}}) = \frac{1}{n_{MC}} \sum_{i=1}^{n_{MC}} \mathbb{1}_{\mu_n(\mathbf{x}_i) \leq 0}(\mathbf{X}_i) \quad (9)$$

In the currently available methods, the part of failure probability variance due to the GP is neglected as the learning criteria are conceived to build a very

confident GP model in terms of classification accuracy, which justifies the use
 140 of the mean $\mu_n(\mathbf{X}_i)$ of the GP predictor in the estimator's expression given
 by Eq. (9). In fact, learning stopping conditions are in general very conserva-
 tive, which probably leads to an overquality of the GP when compared to the
 sampling variance.

In the next section, we provide new measures of the influence on the proba-
 145 bility of failure of the use of numerical integration by MCS and surrogate model
 approximations based on a variance decomposition.

3. Measure of failure probability sensitivity to GP and MC estimation uncertainties

Some investigations to take into account the GP accuracy on a quantity of
 150 interest have been carried out. For example, Le Gratiet proposed in [33] to
 provide confidence intervals of Sobol indices estimated by GP regression and
 Monte Carlo integration. Therefore, a quantification of the contribution of both
 uncertainty sources to the Sobol indices estimators variability is proposed in [33].
 In [34, 35], a learning function is proposed that is based on the contribution of a
 155 point of the MC population, considering the dependencies to other samples, to
 the error of the failure probability estimation. In [14], Schöbi proposed to use
 bounds of the probability of failure estimator \hat{P}_f in an active learning algorithm
 for reliability analysis to define a learning stopping condition. In Schöbi's work,
 the bounds were computed by classifying the points of the population using
 160 their prediction bound values.

3.1. Variance decomposition

To consider the Gaussian process uncertainties, the failure probability can
 be rewritten in the following way :

$$\begin{aligned}
 P_f &= \mathbb{E}_{\mathcal{G}_n, f_{\mathbf{X}}} [\mathbb{1}_{\mathcal{G}_n(\mathbf{X}) \leq 0}] \\
 &= \int_{\Omega_P} \int_{\mathbb{R}^m} \mathbb{1}_{g_n(\mathbf{x}) \leq 0} f_{\mathbf{X}}(\mathbf{x}) f_{\mathcal{G}_n}(g_n) d\mathbf{x} dg_n
 \end{aligned} \tag{10}$$

where Ω_P is the set of conditioned GP trajectories denoted by \mathcal{G}_n and $f_{\mathcal{G}_n}$ is the conditioned GP distribution. The Monte Carlo probability of failure estimator \hat{P}_f^t is then given by

$$\hat{P}_f^t = \frac{1}{n_t} \frac{1}{n_{MC}} \sum_{i=1}^{n_t} \sum_{j=1}^{n_{MC}} \mathbb{1}_{G_i(\mathbf{X}_{i,j}) \leq 0}(\mathbf{X}_{i,j}) = \frac{1}{n_t} \sum_{i=1}^{n_t} \hat{P}_f(G_i, \tilde{\mathbf{X}}_i) \quad (11)$$

where G_i are i.i.d. random processes of the conditioned GP with the same distribution as \mathcal{G}_n and $\tilde{\mathbf{X}}_i$ are n_{MC} -sized sample of \mathbf{X} , that is $\tilde{\mathbf{X}}_i = (\mathbf{X}_{i,j})_{j=1, \dots, n_{MC}}$. The random variables $\hat{P}_f(G_i, \tilde{\mathbf{X}}_i)$ are i.i.d. with the same distribution as $\hat{P}_f(\mathcal{G}_n, \tilde{\mathbf{X}})$, that is the failure probability estimator for a GP \mathcal{G}_n and an n_{MC} -sized Monte Carlo sample $\tilde{\mathbf{X}}$:

$$\hat{P}_f(\mathcal{G}_n, \tilde{\mathbf{X}}) = \frac{1}{n_{MC}} \sum_{i=1}^{n_{MC}} \mathbb{1}_{\mathcal{G}_n(\mathbf{X}_i) \leq 0}(\mathbf{X}_i) \quad (12)$$

This rewriting of the probability of failure estimator allows to explicitly express it as depending on two random variables, $\tilde{\mathbf{X}}$ related to the Monte Carlo sampling uncertainty and \mathcal{G}_n related to the GP approximation uncertainty. 165

In order to assess the contributions of each of both uncertainty sources $\tilde{\mathbf{X}}$ and \mathcal{G}_n on the variance of \hat{P}_f separately, we can refer to the variance decomposition expression [36] which is a classical tool in sensitivity analysis:

$$Var_{\mathcal{G}_n, \tilde{\mathbf{X}}}(\hat{P}_f(\mathcal{G}_n, \tilde{\mathbf{X}})) = V_{\tilde{\mathbf{X}}} + V_{\mathcal{G}_n} + V_{\mathcal{G}_n, \tilde{\mathbf{X}}} \quad (13)$$

where:

- $V_{\tilde{\mathbf{X}}} = Var_{\tilde{\mathbf{X}}}(\mathbb{E}_{\mathcal{G}_n}[\hat{P}_f|\tilde{\mathbf{X}}])$ measures the influence of the Monte Carlo sampling on the variance of \hat{P}_f ,
- $V_{\mathcal{G}_n} = Var_{\mathcal{G}_n}(\mathbb{E}_{\tilde{\mathbf{X}}}[\hat{P}_f|\mathcal{G}_n])$ measures the influence of the GP uncertainty on the variance of \hat{P}_f , 170
- $V_{\mathcal{G}_n, \tilde{\mathbf{X}}} = Var_{\mathcal{G}_n, \tilde{\mathbf{X}}}(\mathbb{E}[\hat{P}_f|\mathcal{G}_n, \tilde{\mathbf{X}}]) - V_{\mathcal{G}_n} - V_{\tilde{\mathbf{X}}}$ measures the joint contribution of both Monte Carlo and GP uncertainties on the variance of \hat{P}_f .

3.2. Variance contributions estimation

175 As the GP enrichment points are chosen among the MC population, $\tilde{\mathbf{X}}$ and \mathcal{G}_n are theoretically not independent. However, as the samples of the MC population used to learn the GP only represent a small part of the population. The estimators developed in the next sections are based on an independence hypothesis.

180 3.2.1. Variance estimator

Let us assume we have a random i.i.d sample of size n_s (Z_1, \dots, Z_{n_s}) of a random variable Z following an unknown distribution. The mean of Z is approached by the empirical mean over the n_s samples denoted by $\overline{Z_{n_s}}$. The empirical variance of a random vector Z , denoted $\widehat{Var}(Z)$ throughout the paper, is defined by:

$$\widehat{Var}(Z) = \frac{1}{n_s - 1} \sum_{i=1}^{n_s} (Z_i - \overline{Z_{n_s}})^2 \quad (14)$$

The estimated asymptotic confidence interval $[\widehat{Var}^{inf}(Z), \widehat{Var}^{sup}(Z)]$ of the variance of level $1 - \alpha$ is given according to the central limit theorem by:

$$\left[\widehat{Var}(Z) - k \frac{\sqrt{n_s \widehat{Var}((Z_i - \overline{Z_{n_s}})^2)}}{n_s - 1}; \widehat{Var}(Z) + k \frac{\sqrt{n_s \widehat{Var}((Z_i - \overline{Z_{n_s}})^2)}}{n_s - 1} \right] \quad (15)$$

where k is the quantile of order $1 - \alpha$ of the reduced centred normal distribution.

3.2.2. Expression of $V_{\tilde{\mathbf{X}}}$ estimator

185 First let us recall that the random variable $Y = \mathbb{1}_{\mathcal{G}_n(\mathbf{x}) \leq 0}(\mathbf{x})$ is a Bernoulli random variable $\mathcal{B}(p(\mathbf{x}))$ with parameter $p(\mathbf{x}) = \mathbb{P}[\mathcal{G}_n(\mathbf{x}) \leq 0] = \Phi\left(-\frac{\mu_n(\mathbf{x})}{\sigma_n(\mathbf{x})}\right)$, the probability that \mathbf{x} belongs to the failure domain according to the Gaussian process \mathcal{G}_n .

The expected value of \hat{P}_f , given by Eq. (12), knowing a Monte Carlo population of n_{MC} samples $\tilde{\mathbf{X}} = (\mathbf{X}_i)_{i=1, \dots, n_{MC}}$ can be expressed as follows:

190

$$\begin{aligned}\mathbb{E}_{\mathcal{G}_n} \left[\hat{P}_f | \tilde{\mathbf{X}} \right] &= \mathbb{E}_{\mathcal{G}_n} \left[\frac{1}{n_{MC}} \sum_{i=1}^{n_{MC}} \mathbb{1}_{\mathcal{G}_n(\mathbf{X}_i) \leq 0}(\mathbf{X}_i) | (\mathbf{X}_i)_{i=1, \dots, n_{MC}} \right] \\ &= \frac{1}{n_{MC}} \sum_{i=1}^{n_{MC}} p(\mathbf{X}_i)\end{aligned}\quad (16)$$

Using the analytical expression of $\mathbb{E}_{\mathcal{G}_n} \left[\hat{P}_f | \tilde{\mathbf{X}} \right]$ given by Eq. (16), the variance $V_{\tilde{\mathbf{X}}}$ can then be obtained by simulating:

$$V_{\tilde{\mathbf{X}}} = \text{Var}_{\tilde{\mathbf{X}}} \left(\frac{1}{n_{MC}} \sum_{i=1}^{n_{MC}} p(\mathbf{X}_i) \right) = \frac{\text{Var}_{\tilde{\mathbf{X}}}(p(\mathbf{X}))}{n_{MC}} \quad (17)$$

The last equality is obtained as $p(\mathbf{X})$ is a continuous random variable between 0 and 1 and $p(\mathbf{X}_i)$ are i.i.d replications of it.

In practice, Eq. (17) is estimated on the Monte Carlo population used for the estimation of the probability of failure. Hence the estimator of $V_{\tilde{\mathbf{X}}}$, denoted by $\widehat{V}_{\tilde{\mathbf{X}}}$, on a MC population realization is given by:

$$\widehat{V}_{\tilde{\mathbf{X}}} = \frac{\widehat{\text{Var}}_{\tilde{\mathbf{X}}}(p(\tilde{\mathbf{X}}))}{n_{MC}} = \frac{1}{n_{MC}(n_{MC} - 1)} \sum_{i=1}^{n_{MC}} \left(p(\mathbf{X}_i) - \frac{1}{n_{MC}} \sum_{j=1}^{n_{MC}} p(\mathbf{X}_j) \right)^2 \quad (18)$$

and its $1 - \alpha$ confidence interval estimated bounds can be expressed using Eq. (15) and are given by:

$$\begin{aligned}\widehat{V}_{\tilde{\mathbf{X}}}^{inf} &= \frac{\widehat{\text{Var}}_{\tilde{\mathbf{X}}}^{inf}(p(\tilde{\mathbf{x}}))}{n_{MC}} \\ \widehat{V}_{\tilde{\mathbf{X}}}^{sup} &= \frac{\widehat{\text{Var}}_{\tilde{\mathbf{X}}}^{sup}(p(\tilde{\mathbf{x}}))}{n_{MC}}\end{aligned}\quad (19)$$

3.2.3. Expression of $V_{\mathcal{G}_n}$ estimator

The computation of the expected value of \hat{P}_f knowing a realization of \mathcal{G}_n can be interpreted as a classical Monte Carlo simulation for a deterministic model. Hence it follows this equality:

$$\mathbb{E}_{\tilde{\mathbf{X}}} \left[\hat{P}_f | \mathcal{G}_n \right] = \mathbb{E}_{\tilde{\mathbf{X}}} \left[\frac{1}{n_{MC}} \sum_{i=1}^{n_{MC}} \mathbb{1}_{\mathcal{G}_n(\mathbf{x}_i) \leq 0}(\mathbf{X}_i) | \mathcal{G}_n \right] \quad (20)$$

$$= P_f(\mathcal{G}_n) \quad (21)$$

with $P_f(\mathcal{G}_n)$ the probability of failure for a realization of \mathcal{G}_n . Classically, this probability of failure is approached by a Monte Carlo estimator $\hat{P}_f^{MC}(\mathcal{G}_n) = \frac{1}{n_{MC}} \sum_{i=1}^{n_{MC}} \mathbb{1}_{\mathcal{G}_n(\mathbf{X}_i) \leq 0}(\mathbf{X}_i)$, with $(\mathbf{X}_i)_{i=1, \dots, n_{MC}}$ a Monte Carlo population realization. Hence, $V_{\mathcal{G}_n}$ can be numerically estimated by simulating different trajectories of \mathcal{G}_n and computing the Monte Carlo estimator of P_f for each simulated trajectory.

Let $(G_i)_{1 \leq i \leq n_t}$ be n_t realizations of \mathcal{G}_n , then the $V_{\mathcal{G}_n}$ estimate is the empirical variance of the sample $\hat{P}_f^{MC}(G_i)_{1 \leq i \leq n_t}$:

$$\widehat{V}_{\mathcal{G}_n} = \widehat{Var}_{\mathcal{G}_n}(\hat{P}_f^{MC}(\mathcal{G}_n)) = \frac{1}{n_t - 1} \sum_{i=1}^{n_t} \left(\hat{P}_f^{MC}(G_i) - \frac{1}{n_t} \sum_{i=1}^{n_t} \hat{P}_f^{MC}(G_i) \right)^2 \quad (22)$$

Moreover its $1 - \alpha$ confidence interval estimated bounds, also expressed using Eq. (15), are given by:

$$\begin{aligned} \widehat{V}_{\mathcal{G}_n}^{inf} &= \widehat{Var}_{\mathcal{G}_n}^{inf}(\hat{P}_f^{MC}(\mathcal{G}_n)) \\ \widehat{V}_{\mathcal{G}_n}^{sup} &= \widehat{Var}_{\mathcal{G}_n}^{sup}(\hat{P}_f^{MC}(\mathcal{G}_n)) \end{aligned} \quad (23)$$

In practice, the computation of conditioned GP realizations is prone to numerical issues. In Appendix A, these numerical issues and their sources are exposed and an alternative method, presented in [33, 37], based on the simulation of an unconditioned Gaussian process is detailed.

3.2.4. Expression of the total variance estimator

The total variance of \hat{P}_f can then be estimated with:

$$\widehat{V}_{tot} = \widehat{Var}_{\mathcal{G}_n, \tilde{\mathbf{X}}}(\hat{P}_f(\mathcal{G}_n, \tilde{\mathbf{X}})) = \frac{1}{n_t - 1} \sum_{i=1}^{n_t} \left(\hat{P}_f(G_i, \tilde{\mathbf{X}}_i) - \frac{1}{n_t} \sum_{j=1}^{n_t} \hat{P}_f(G_j, \tilde{\mathbf{X}}_j) \right)^2 \quad (24)$$

where $(G_i, \tilde{\mathbf{X}}_i)$, $i = 1, \dots, n_t$ are n_t realizations of \mathcal{G}_n and Monte Carlo population $\tilde{\mathbf{X}}$ and $\hat{P}_f(G_i, \tilde{\mathbf{X}}_i)$ is the probability of failure estimation for the i^{th} realization $(G_i, \tilde{\mathbf{X}}_i)$ of \mathcal{G}_n and $\tilde{\mathbf{X}}$. \widehat{V}_{tot} is the empirical variance of the sample $(\hat{P}_f(G_i, \tilde{\mathbf{X}}_i))_{1 \leq i \leq n_t}$.

Moreover the $1 - \alpha$ confidence interval estimated bounds of \widehat{V}_{tot} , also expressed using the operators defined in Eq. (15), are given by:

$$\begin{aligned}\widehat{V}_{tot}^{inf} &= \widehat{Var}_{\mathcal{G}_n, \tilde{\mathbf{X}}}^{inf}(\hat{P}_f(\mathcal{G}_n, \tilde{\mathbf{X}})) \\ \widehat{V}_{tot}^{sup} &= \widehat{Var}_{\mathcal{G}_n, \tilde{\mathbf{X}}}^{sup}(\hat{P}_f(\mathcal{G}_n, \tilde{\mathbf{X}}))\end{aligned}\quad (25)$$

In practice, the numerical cost of the n_t estimations of $\hat{P}_f(G_i, \tilde{\mathbf{X}}_i) = \hat{P}_f(G_i(\tilde{\mathbf{X}}_i))$ can be quite high to get a sufficiently low variance of the estimator \widehat{V}_{tot} . Hence, we propose to use a bootstrap procedure [38] to simulate several MC populations $\tilde{\mathbf{X}}_i$ from the population $\tilde{\mathbf{X}}$ on which the n_t GP trajectories are computed [33]. Bootstrap is applicable here as we assume that the size n_{MC} is sufficiently large to consider that sampling with the empirical distribution or with the true distribution is similar. The method proposed to estimate the $\hat{P}_f(G_i, \tilde{\mathbf{X}}_i)$ is presented in Algorithm 1.

Algorithm 1 Evaluation process of $\hat{P}_f(G_i, \tilde{\mathbf{X}}_i)$ via n_t bootstrap samples

Require: $\tilde{\mathbf{X}}, \mathcal{G}_n, n_t$

- 1: Simulation of $i = 1, \dots, n_t$ trajectories $G_i(\tilde{\mathbf{X}}) = (G_i(\mathbf{X}_j))_{j=1, \dots, n_{MC}}$ of \mathcal{G}_n at MC population samples $\tilde{\mathbf{X}}$
 - 2: **for** $i = 1, \dots, n_t$ **do**
 - 3: Sampling with replacement of a sample \mathbf{Z} of size n_{MC} from $\tilde{\mathbf{X}}$
 - 4: Extract values of $G_i(\mathbf{Z})$ from $G_i(\tilde{\mathbf{X}})$
 - 5: Estimation of $\hat{P}_f(G_i, \tilde{\mathbf{X}}_i)$ using Eq. (12) with $\tilde{\mathbf{X}}_i = \mathbf{Z}$ and $G_i(\tilde{\mathbf{X}}_i) = G_i(\mathbf{Z})$
 - 6: **end for**
 - 7: **return** Estimation of $(\hat{P}_f(G_i, \tilde{\mathbf{X}}_i))_{i \in 1, \dots, n_t}$
-

Finally, the probability of failure is estimated by the mean over the $(\hat{P}_f(G_i, \tilde{\mathbf{X}}_i))_{1 \leq i \leq n_t}$, i.e. by:

$$\hat{P}_f^t = \frac{1}{n_t} \sum_{i=1}^{n_t} \hat{P}_f(G_i, \tilde{\mathbf{X}}_i) \quad (26)$$

Hence, estimated total COV, denoted by COV_{tot} , of an estimation \hat{P}_f^{MC} of the probability of failure \hat{P}_f obtained on a MC realization is thus given by:

$$\widehat{COV}_{tot} = \frac{\sqrt{\widehat{V}_{tot}}}{\hat{P}_f^t} \quad (27)$$

Its $1 - \alpha$ confidence interval estimated bounds are then estimated by:

$$\begin{aligned} \widehat{COV}_{tot}^{inf} &= \frac{\sqrt{\widehat{V}_{tot}^{inf}}}{\hat{P}_f^t} \\ \widehat{COV}_{tot}^{sup} &= \frac{\sqrt{\widehat{V}_{tot}^{sup}}}{\hat{P}_f^t} \end{aligned} \quad (28)$$

Finally notice that the joint contribution of the MC integration and the GP approximation uncertainties $V_{G_n, \bar{X}}$ can then be estimated by computing the three previous estimators and applying the relation given by Eq. (13). By carrying out this calculation the independence hypothesis introduced at the beginning of Sec. 3.2 can be empirically verified.

3.3. Motivation for developing a new adaptive sampling approach illustrated on a benchmark case

The idea here is to explain our motivation to propose a new approach in order to perform a trade-off between improving the GP and adding points to the MCS. To illustrate this point, a well known benchmark example is chosen.

The application deals with the example of a series system with four branches limit state introduced in [39] and chosen for its high non-linearity and rather complex limit state. The random variables X_1 and X_2 follow standard normal distributions. The performance function is given by:

$$y = \min_{x_1, x_2} \left\{ \begin{array}{l} 3 + 0.1(x_1 - x_2)^2 - \frac{(x_1 + x_2)}{\sqrt{(2)}}; \\ 3 + 0.1(x_1 - x_2)^2 + \frac{(x_1 + x_2)}{\sqrt{(2)}}; \\ (x_1 - x_2) + \frac{6}{\sqrt{2}}; \\ (x_2 - x_1) + \frac{6}{\sqrt{2}} \end{array} \right\} \quad (29)$$

A run of the AK-MCS+*EFF* algorithm gives an estimation of P_f and the corresponding MC coefficient of variation. In this example, this algorithm was

run with an initial Monte Carlo population of size 10^4 and a maximum allowed coefficient of variation of 5%. At each iteration of the algorithm, the variability
 240 due to the GP \mathcal{G}_n and the Monte Carlo based integration $\tilde{\mathbf{X}}$ was estimated using respectively Eq. (22) and Eq. (18). To visualize the GP uncertainty, Fig. 1 shows three different trajectories of the limit state approximation drawn from a GP constructed from a DoE of 50 points. It can be seen that the three trajectories are relatively close to each other in areas that contribute a lot to the probability
 245 of failure but there is large variability among the three trajectories in areas (i.e. the four corners), that contribute little to the probability of failure (cf. also to Fig. 5a to visualize the Monte Carlo samples). Our variance estimator of Eq. (22) quantifies the variance of the \hat{P}_f estimator associated with the different possible trajectories of the GP, while the variance estimator of Eq. (18) quantifies the variance of the \hat{P}_f estimator associated with different possible samples for the
 250 MCS.

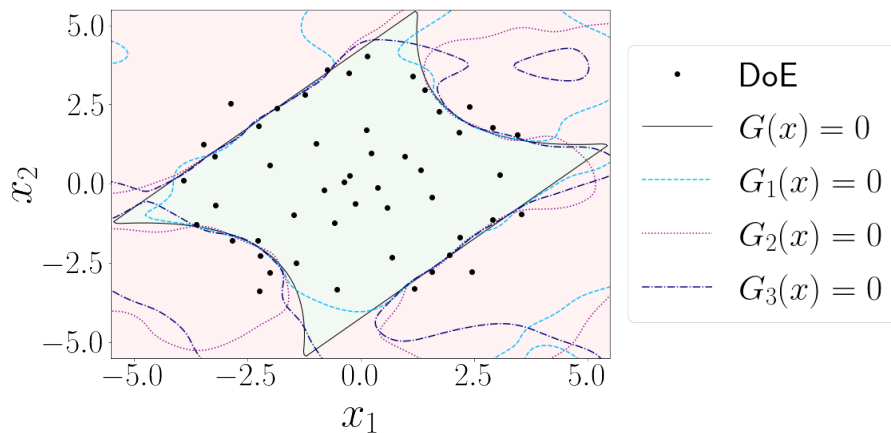


Figure 1: Four branches test case: true limit state function $G(x) = 0$ and three trajectories approximating it, drawn from the GP constructed based on 50 DoE points.

The evolution of the probability of failure and the corresponding variance estimations throughout the algorithm are respectively illustrated on Fig. 2 and Fig. 3.

255 In particular, it can be seen on Fig. 3 that for the 18 first iterations the

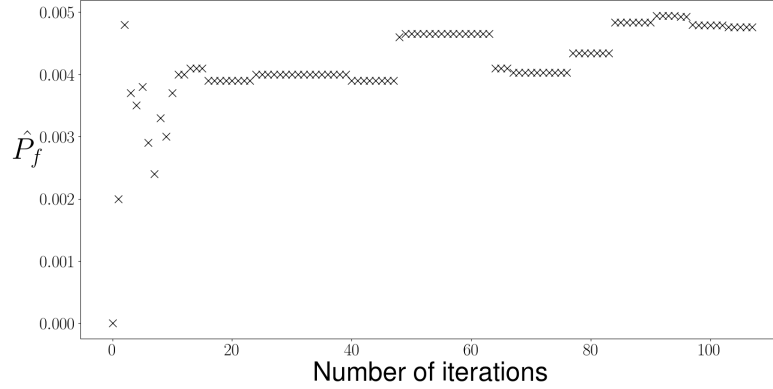


Figure 2: Evolution of the probability of failure estimation as a function of the number of iterations throughout a run of the algorithm $AK-MCS+EFF$ ($\hat{P}_f^{MC} = 4.46 \times 10^{-3}$ ($COV = 1.6\%$)) on the four branches test case.

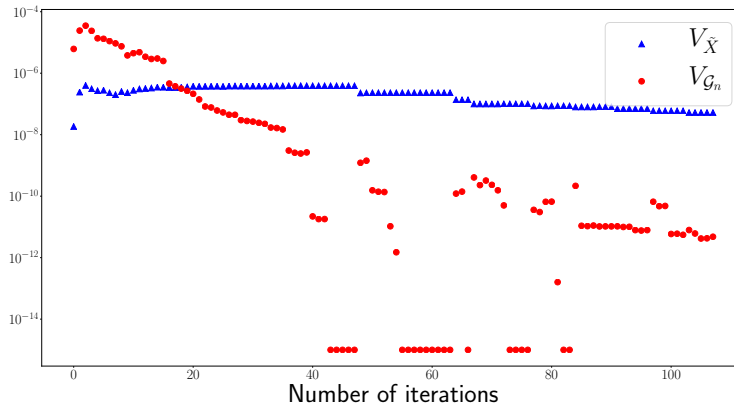


Figure 3: Evolution of the variances $V_{\hat{X}}$ and $V_{\mathcal{G}_n}$ estimations as a function of the number of iterations throughout a run of the algorithm $AK-MCS+EFF$ on the four branches test case.

main contributor to the failure probability variance is the GP \mathcal{G}_n . Then, until the end of the run the principal source of variability is the Monte Carlo integration. However, the GP is still enriched after the 18th iteration of this algorithm reaching 99 enrichment points when the algorithm converges. Moreover, it can
 260 be seen on Fig. 2 that the spread of \hat{P}_f estimation values stops around the 15th

iteration and progresses then in the vicinity of the true value of the probability of failure. At the end of the run, the part of variability on \hat{P}_f due to the Monte Carlo integration is 1.1×10^4 higher than the one attributed to the GP approximation.

265 The variance comparison leads us to conclude that there is no need to learn the GP in a so accurate way and by avoiding this we can hope to save some unnecessary simulations of the performance function.

Hence, it could be interesting to integrate these measures of variance in the learning procedure to overcome the over-conservative learning of GP. The 270 proposed method is detailed in the next section.

4. Proposed method

4.1. General concept

The new method consists in using the variance estimations obtained previously in the learning phase as decision criteria of a novel, adaptive enrichment 275 process for probability of failure approximation. On the one hand, the contributions attributed to the Monte Carlo estimation and the GP to the variability of \hat{P}_f can be used to decide whether to improve the GP or to increase the size of the sampling population. These contributions can be quantified using the variances estimators given by Eq. (18) for the MC integration contribution and 280 by Eq. (22) for the GP approximation. On the other hand, the total variance on \hat{P}_f , whose estimator is given by Eq. (24), can be used as a criterion to stop the learning phase.

4.2. Proposed algorithm

The proposed Variance based Active GP (Vb-AGP) learning procedure is 285 summarized in Fig. 4 and the different stages are described below:

1. Generation of an initial Monte Carlo population $\tilde{\mathbf{X}}$ of n_{MC} samples.
2. Initial Design of Experiments (DoE) of n samples defined using sampling methods such as Latin Hypercube Sampling (LHS). The performance function $G(\mathbf{x})$ is then evaluated at the n samples.

- 290 3. Construction of a GP metamodel $\mathcal{G}_n(\mathbf{x})$ of the performance function $G(\mathbf{x})$ on the DoE.
4. Estimation of the failure probability P_f on the Monte Carlo population $\tilde{\mathbf{X}}$ according to the following equation:

$$\hat{P}_f^{MC}(\tilde{\mathbf{X}}) = \frac{1}{n_{MC}} \sum_{i=1}^{n_{MC}} \mathbb{1}_{\mu_n(\mathbf{x}_i) \leq 0} \quad (30)$$

5. Interval estimation of variances $V_{\tilde{\mathbf{X}}}$ and $V_{\mathcal{G}_n}$ using respectively Eq. (19) and Eq. (23).

295 Note that we seek to obtain $\left[\widehat{V_{\tilde{\mathbf{X}}}^{inf}}, \widehat{V_{\tilde{\mathbf{X}}}^{sup}} \right] \cap \left[\widehat{V_{\mathcal{G}_n}^{inf}}, \widehat{V_{\mathcal{G}_n}^{sup}} \right] = \emptyset$, using the estimators given in Sec. 3.2, in order to compare both variance values. Therefore new GP trajectories have to be simulated until the estimation of $V_{\mathcal{G}_n}$ confidence interval is sufficiently narrow.

6. Compute $\widehat{COV}_{red} = \frac{\sqrt{\widehat{V_{\mathcal{G}_n}^{sup}} + \widehat{V_{\tilde{\mathbf{X}}}^{sup}}}}{\hat{P}_f^{MC}}$.
- 300 If $\widehat{COV}_{red} < COV_{max}$, with COV_{max} a user defined maximum allowed total coefficient of variation, the algorithm goes to step 7 to verify that the total COV is below the maximum allowed value.
- Otherwise, the algorithm goes to step 8 in order to reduce the main source of uncertainty.

7. Interval estimation of the total coefficient of variation COV_{tot} using Eq. (28):
- 305 increasing number of simulations until $COV_{max} \notin \left[\widehat{COV}_{tot}^{inf}, \widehat{COV}_{tot}^{sup} \right]$. If $COV_{tot}^{sup} \leq COV_{max}$ then the estimation \hat{P}_f^t of P_f with Eq. 26 is considered sufficiently accurate and the algorithm is stopped.

Otherwise, the algorithm goes to the next step.

- 310 8. If $\widehat{V_{\mathcal{G}_n}} < \widehat{V_{\tilde{\mathbf{X}}}}$, new samples are added to the Monte Carlo population and the method goes back to step 4 to update the estimation of P_f .

Else if $\widehat{V_{\mathcal{G}_n}} > \widehat{V_{\tilde{\mathbf{X}}}}$, the algorithm goes to step 9.

9. The learning function $EFF(\mathbf{x})$ given by Eq. (8) is evaluated on the whole MC population to find the best candidate \mathbf{x}^* to evaluate for enriching the
- 315 GP metamodel. The performance function is computed on the sample \mathbf{x}^*

and the DoE is enriched with this new point \mathbf{x}^* . Then the method goes to step 3 to update the GP model.

The first stage of the stopping condition on learning consists in verifying the following equation:

$$\widehat{COV}_{red} = \frac{\sqrt{\widehat{V}_{G_n}^{sup} + \widehat{V}_X^{sup}}}{\widehat{P}_f^{MC}} < COV_{max} \quad (31)$$

where COV_{max} is a user defined maximum allowed total coefficient of variation,

The condition given by Eq. (31) corresponds to a condition on the approx-
 320 imation of the total variance of the \widehat{P}_f , under the independence assumption. Indeed, throughout the learning, the joint contribution of both variables is never computed, since it would significantly increase the computational cost. If Eq. (31) is verified, the total variance V_{tot} including the joint contribution can be estimated (i.e. in step 7 of the algorithm) to make sure that it respects
 325 the maximum variance allowed.

Let us now make a few comments about the choices made for this algo-
 rithm. First we have found that the learning function $EFF(\mathbf{x})$ appears better
 suited than $U(\mathbf{x})$. Indeed, the learning function $EFF(\mathbf{x})$ tends to explore more,
 whereas the function $U(\mathbf{x})$ focuses on a very accurate learning of the currently
 330 known limit state before exploring the rest of the domain.

Finally, note that seeking to equalize the two variance contributions $V_{\widehat{\mathbf{X}}}$ and
 V_{G_n} is not guaranteed to be the most computationally cost efficient strategy.
 The optimal strategy will be problem dependent, however seeking equal contri-
 butions of the two variances $V_{\widehat{\mathbf{X}}}$ and V_{G_n} appears as a good general guideline
 335 and, in most cases, the corresponding computational cost is expected to be quite
 close to the actual optimum.

4.3. Applications

4.3.1. Methodology settings and comparison measures

It has been observed in many numerical applications that the squared-
 340 exponential kernel, also called Gaussian correlation model, is likely to undergo

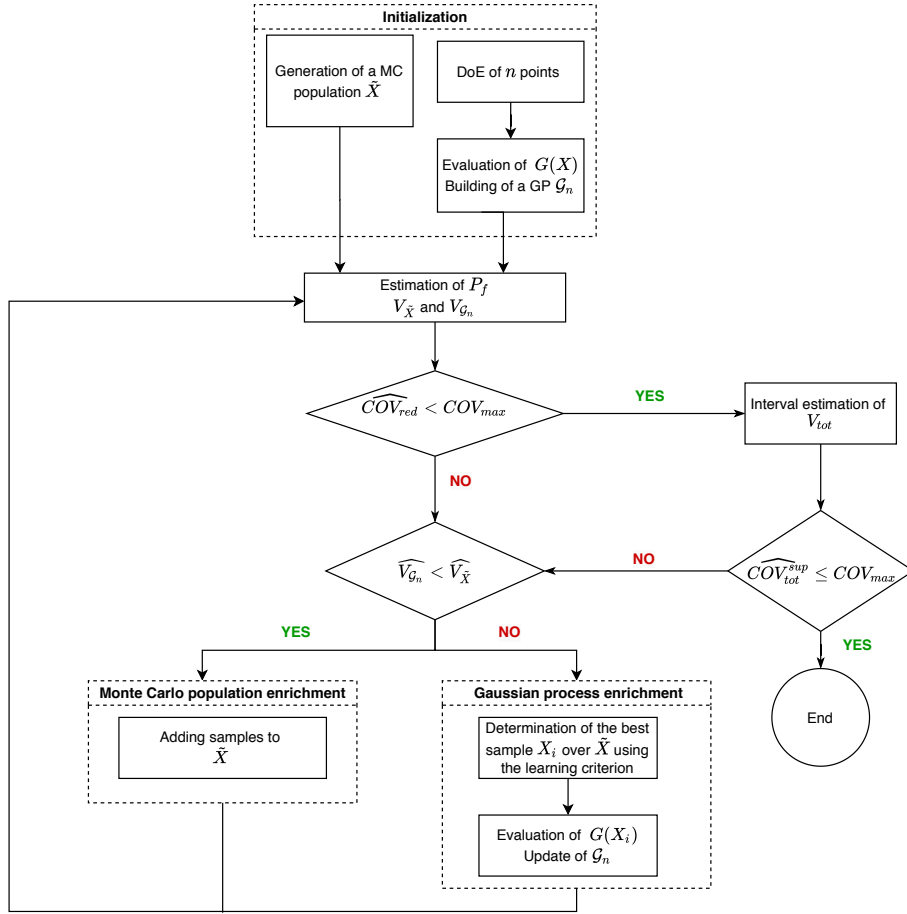


Figure 4: Flowchart of the learning algorithm Vb-AGP + MCS.

ill-conditioning [40]. For this reason, in this paper the Matérn $5/2$ kernel will be used.

Moreover, as for the AK methods, a maximum allowed COV has to be set as a stopping criterion of the algorithm. However, the COV computed in the
345 proposed algorithm includes all uncertainties (not only the MC ones) and the method is built to have balanced amount of variability due to both sources of uncertainty. This must be taken in consideration when choosing the value of COV_{max} .

The different active learning methods performances comparison can be based

350 on different criterion or error measures such as:

- $COV(\hat{P}_f)$: the COV of \hat{P}_f estimations obtained on n_{run} independent runs of the estimation procedure of P_f ;
- e_r : the mean over the n_{run} values of the absolute relative error between the estimations $\hat{P}_{f_i}, i = 1, \dots, n_{run}$ obtained and a reference value $P_{f_{ref}}$ (obtained e.g. by MCS with a very large number of samples)

$$e_r = \frac{1}{n_{run}} \sum_{i=1}^{n_{run}} \frac{|\hat{P}_{f_i} - P_{f_{ref}}|}{P_{f_{ref}}} \quad (32)$$

- ν_{MC} : a coefficient allowing to compare the numerical efficiency of the considered method to a classical MCS method, that is defined as follows:

$$\nu_{MC} = \frac{N_{call}^{MC}}{N_{call}} \quad (33)$$

where N_{call} corresponds to the number of calls of the active learning method to the performance function to reach a COV equal to $COV(\hat{P}_f)$ and N_{call}^{MC} is the number of samples needed by a MCS method (estimated
 355 by Eq. (??)) to obtain the same COV of $COV(\hat{P}_f)$ on the probability of failure.

The efficiency ν_{MC} actually corresponds to the factor dividing the MCS budget to reach the same level of accuracy on P_f with the active learning
 360 based method considered.

4.3.2. Series system with four branches limit state

We have applied the classical AK-MCS and the proposed methods on the example of a series system with a four branches limit state already defined in Sec. 3.3.

365 The proposed method was run for an initial DoE of 16 samples, an initial MC population of 5×10^4 and a maximum coefficient of variation of 3%. The final DoE resulting from a run of AK-MCS+*EFF* and the final DoE obtained with a run of the proposed variance based algorithm on the same initial DoE

and MC population are illustrated respectively on Fig. 5a and Fig. 5b. It can
 370 already be observed on these figures that the proposed variance based algorithm
 adds less points to the DoE to fulfill the learning stopping criterion.

The variations of both variance estimators $V_{\hat{\mathbf{x}}}$ and $V_{\mathcal{G}_n}$ during a run are
 provided in Fig. 6.

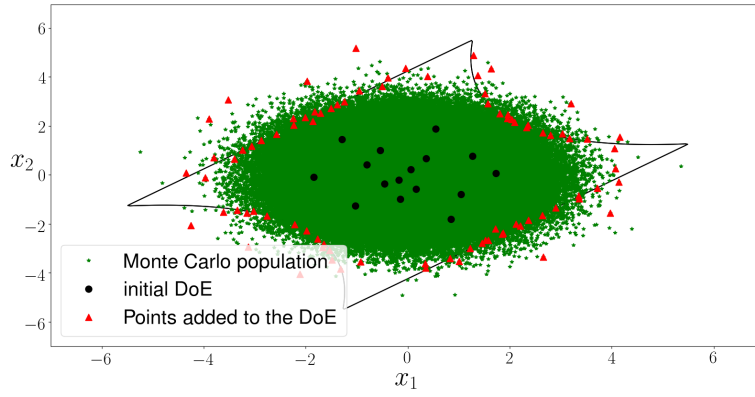
As for the algorithm AK-MCS, the influence of the GP is predominant at the
 375 beginning of the run and the surrogate model has to be enriched. However, we
 can see that at the end of the run the values of $V_{\hat{\mathbf{x}}}$ and $V_{\mathcal{G}_n}$ are more balanced
 and $V_{\mathcal{G}_n}$ is not much lower than $V_{\hat{\mathbf{x}}}$. Nonetheless, the estimated total COV at
 the end of the run is 2.9% and respects thus the allowed COV of 3%. Here,
 the quantity $\frac{\sqrt{V_{\hat{\mathbf{x}}}}}{\hat{P}_f}$ corresponding to the MC COV, that is usually used as a
 380 variability measure, is equal to 2.1%.

Then the algorithm was run 100 times with different initial DoEs of 16
 points and initial Monte Carlo populations of 5×10^4 . A maximum coefficient
 of variation of 3% was set. The reference result obtained, on average, by 100
 runs of MCS ($n_{MC} = 10^6$) and the mean results of all methods are presented
 385 in Tab. 1.

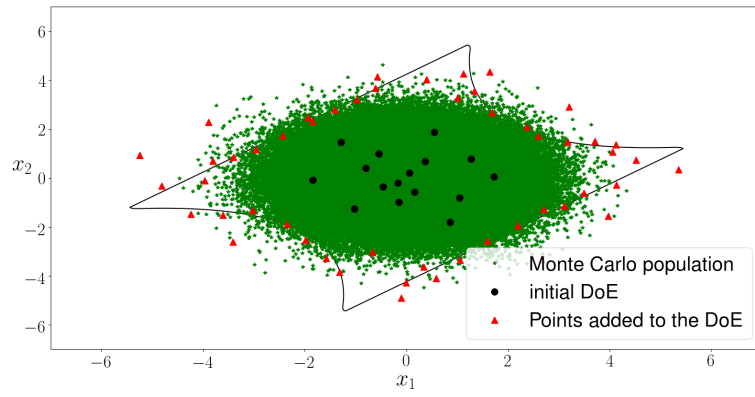
Method	N_{call}	$COV(N_{call})$	\hat{P}_f	$COV(\hat{P}_f)$	e_r	ν_{MC}
MCS	10^6	-	4.46×10^{-3}	1.6%	-	-
AK-MCS + U	128	6.6%	4.48×10^{-3}	3%	2.4%	1976
AK-MCS + EFF	144	6.6%	4.46×10^{-3}	3%	2.5%	1690
Vb-AGP + MCS	68	9.0%	4.46×10^{-3}	2.6%	2.0%	5146

Table 1: Series system with four branches— 100 run mean results - Adaptive method param-
 eters: $n_{MC}^{init} = 5 \times 10^4$, $n_{DoE}^{init} = 16$, $COV_{max} = 0.03$.

The results show that the method Vb-AGP allows to reduce the number of
 learning points needed to respect the same accuracy. Moreover, we can see that
 the variance (respectively COV) estimator proposed in this work is consistent
 with the empirical variance obtained on 100 runs of the algorithm. Indeed, the



(a) AK-MCS+*EFF* result



(b) Vb-AGP + MCS approach result

Figure 5: Comparisons of two DoEs: a) resulting from a run of AK-MCS+*EFF* and b) one obtained with a run of the proposed method for the same initial DoE and MC population with COV_{max} set to 3% on the series system with four branches example.

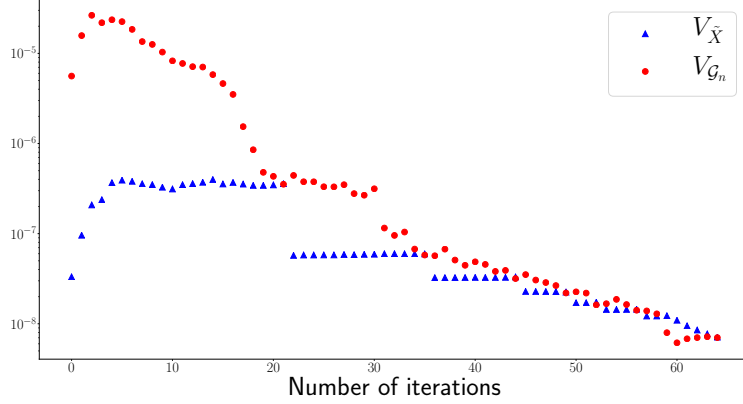


Figure 6: Evolution of the variance $V_{\tilde{X}}$ and V_{G_n} estimations as a function of the number of iterations throughout a run of the proposed algorithm on the four branches test case.

390 maximal imposed COV value is 3% and an empirical COV of 2.6% is obtained. The value of the numerical efficiency indicator ν_{MC} of the proposed method is 3 times higher than for AK-MCS+EFF and 2.6 times higher than for AK-MCS+U.

4.3.3. Dynamic response of an oscillator

395 The example of an oscillator leading to a non-linear limit state function is also widely used in the litterature and concerns the dynamic response of the undamped single degree-of-freedom system illustrated in Fig. 7. This example is also studied in [41, 5, 19].

The corresponding performance function is expressed as:

$$G(C_1, C_2, M, R, T_1, F_1) = 3R - \left| \frac{2F_1}{M\omega_0^2} \sin\left(\frac{\omega_0 T_1}{2}\right) \right| \quad (34)$$

with $\omega_0 = \sqrt{(C_1+C_2)/M}$. Six random Variables listed in Tab. 2 are considered for
 400 this problem. Actually, two cases are proposed here with a change of the applied force F_1 probability distribution parameters which lead to different probability of failure orders of magnitude.

The proposed method and AK-MCS were applied on the first case with

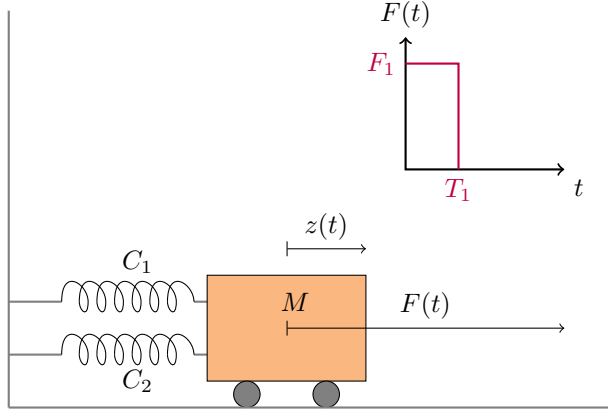


Figure 7: Oscillator with non-linear limit state function.

Variable	Distribution	Mean	standard deviation
C_1	Gaussian	1	0.1
C_2	Gaussian	0.1	0.01
M	Gaussian	1	0.05
R	Gaussian	0.5	0.05
T_1	Gaussian	1	0.2
F_1 – Case 1	Gaussian	1	0.2
F_1 – Case 2	Gaussian	0.6	0.1

Table 2: Random variables for the oscillator test case.

$F_1 \sim \mathcal{N}(1, 0.04)$ corresponding to a reference probability of failure of 2.86×10^{-2}
405 (obtained with 100 runs of MCS with $n_{MC} = 1 \times 10^5$). The methods were run
100 times for an initial DoEs of 12 samples, initial MC populations of 1×10^4
and a maximum coefficient of variation of 3%. The mean results are given in
Tab. 3.

The numerical efficiency indicator ν_{MC} for the proposed method is 1.6 times
410 higher than for AK-MCS + U and 1.8 times higher than for AK-MCS + EFF .

In Tab. 3, the COV of \hat{P}_f estimation is 3.2% on the 100 runs of Vb-AGP
and its 99% confidence interval is given by $[0.022, 0.041]$.

Method	N_{call}	$COV(N_{call})$	\hat{P}_f	$COV(\hat{P}_f)$	ϵ_r	ν_{MC}
MCS	1×10^5	-	2.86×10^{-2}	2%	-	-
AK-MCS + <i>U</i>	59.8	6.4%	2.85×10^{-2}	2.7%	2.2%	792
AK-MCS + <i>EFF</i>	52.5	7.1%	2.87×10^{-2}	2.8%	2.4%	890
Vb-AGP + MCS	22.5	14.4%	2.84×10^{-2}	3.2%	2.6%	1436

Table 3: Result for the oscillator test case ($\mu_{F_1} = 1$, $\sigma_{F_1} = 0.2$) — 100 run mean results
Adaptive method parameters: $n_{MC}^{init} = 10^4$, $n_{DoE}^{init} = 12$, $COV_{max} = 0.03$.

We can see that the COV of the number of calls N_{call} is higher for the method Vb-AGP than for the other enrichment strategies. In this example the number of points added during the learning phase with the proposed method is of the same order of magnitude as the initial DoE. The results obtained are thus dependent on the initial DoE. We can suppose that the number of necessary enrichment points depends on the quality of the initial DoE, in terms of accuracy of the classification, and that is an underlying cause of the higher variance of N_{call} .

As presented previously, another case derived from the oscillator example with another distribution of the variable F_1 can be achieved (Case 2 of Tab. 2). However, this test case corresponds to a very low probability of failure and can thus not be treated with the Vb-AGP + MCS method due to the limits of MCS use for rare events [29]. Therefore, we propose another version of the method that involves Importance Sampling (IS) in order to address low probability of failure problems.

5. Improvement with IS

A way to highly decrease a Monte Carlo based estimator’s variance is to use importance sampling instead of a classical Monte Carlo sampling. Moreover, the use of importance sampling allows to address rare event probabilities as the

number of samples for the integration can be considerably reduced.

5.1. Importance Sampling

The main idea of Importance Sampling (IS) is to find an auxiliary density f_{aux} , well-suited for the estimation of $P_f = \mathbb{P}[G(\mathbf{x}) \leq 0]$, to generate $n_{IS} \ll n_{MC}$ samples $\mathbf{X}_1, \dots, \mathbf{X}_{n_{IS}} \sim f_{aux}$ weighted for the estimation of the sought probability:

$$\hat{P}_f^{IS} = \frac{1}{n_{IS}} \sum_{i=1}^{n_{IS}} w(\mathbf{X}_i) \mathbb{1}_{G(\mathbf{X}_i) \leq 0}(\mathbf{X}_i) \quad (35)$$

with $w(\mathbf{X}_i) = \frac{f_{\mathbf{X}}(\mathbf{X}_i)}{f_{aux}(\mathbf{X}_i)}$ the weight of the sample \mathbf{X}_i . The auxiliary density f_{aux} appears in the computation of the variance of the estimator in the following way:

$$Var\left(\hat{P}_f^{IS}\right) = \frac{Var\left(w(\mathbf{X}_1) \mathbb{1}_{G(\mathbf{X}_1) \leq 0}(\mathbf{X}_1)\right)}{n_{IS}} \quad (36)$$

while the variance of the MC estimator is $\frac{Var(\mathbb{1}_{G(\mathbf{X}_1) \leq 0}(\mathbf{X}_1))}{n_{MC}}$. Hence, if well
 435 chosen, the auxiliary density f_{aux} can considerably reduce the variance of the estimator and improve its convergence. The best possible auxiliary density f_{aux} , denoted f_{aux}^{opt} , is the one that verifies $Var\left(\hat{P}_f^{IS}\right) = 0$. Using Eq. (36), its expression is then given by [42]:

$$f_{aux}^{opt}(\mathbf{x}) = \frac{\mathbb{1}_{G(\mathbf{x}) \leq 0} f_{\mathbf{X}}(\mathbf{x})}{P_f} \quad (37)$$

Since it depends on the probability sought, P_f itself, it cannot be used directly.

440 One of the difficulties of IS is then to compute an auxiliary density f_{aux} as close as possible to f_{aux}^{opt} . Several methods have been developed such as [43, 44, 45]. In this paper, we consider the non parametric adaptive IS (NAIS) proposed in [46] and detailed in Appendix B. The principle of NAIS is to estimate iteratively the density f_{aux}^{opt} with a weighted Gaussian kernel density. The advantage of this
 445 approach is its applicability on relatively complex failure domain as long as the dimensionality of the input is reasonably small ($m < 10$).

The probability of failure estimator obtained when running a GP active learning method combined with IS is given by:

$$\hat{P}_f(\mathcal{G}_n, \mathbf{X}) = \frac{1}{n_{IS}} \sum_{i=1}^{n_{IS}} w_i \mathbb{1}_{\mathcal{G}_n(\mathbf{X}_i) \leq 0}(\mathbf{X}_i) \quad (38)$$

with \mathcal{G}_n the GP of G , $w_i = \frac{f_{\mathbf{X}}(\mathbf{X}_i)}{f_{aux}(\mathbf{X}_i)}$ the weights of the samples generated by IS
 450 and f_{aux} the auxiliary IS density.

The effect of the GP and the IS accuracy on the probability of failure estimate can be obtained by rewriting the indices of variances proposed in Sec. 3.2 adapted for IS.

5.2. Variance based sensitivity index estimations

455 The expected value of \hat{P}_f knowing a population of n_{IS} samples $\tilde{\mathbf{X}} = (\mathbf{X}_i)_{i=1, \dots, n_{IS}}$ generated by IS auxiliary density function f_{aux} can be expressed by rewriting Eq. (16) as follows:

$$\begin{aligned} \mathbb{E}_{\mathcal{G}_n} [\hat{P}_f | \tilde{\mathbf{X}}] &= \mathbb{E}_{\mathcal{G}_n} \left[\frac{1}{n_{IS}} \sum_{i=1}^{n_{IS}} w_i \mathbb{1}_{\mathcal{G}_n(\mathbf{X}_i) \leq 0}(\mathbf{X}_i) | (\mathbf{X}_i)_{i=1, \dots, n_{IS}} \right] \\ &= \frac{1}{n_{IS}} \sum_{i=1}^{n_{IS}} w_i p(\mathbf{X}_i) \end{aligned} \quad (39)$$

Hence, the variance $V_{\tilde{\mathbf{X}}}$ estimator is then obtained by adapting Eq. (18) for IS:

$$\begin{aligned} \widehat{V}_{\tilde{\mathbf{X}}} &= \frac{\widehat{Var}_{\tilde{\mathbf{X}}}((w(\tilde{\mathbf{X}})p(\tilde{\mathbf{X}}))}{n_{IS}} \\ &= \frac{1}{n_{IS}(n_{IS} - 1)} \sum_{i=1}^{n_{IS}} \left(w(\mathbf{X}_i)p(\mathbf{X}_i) - \frac{1}{n_{IS}} \sum_{j=1}^{n_{IS}} w(\mathbf{X}_j)p(\mathbf{X}_j) \right)^2 \end{aligned} \quad (40)$$

460 and its $1 - \alpha$ confidence interval estimated bounds can be expressed similarly to the ones defined in Sec. 3.2.1.

The computation of the expected value of \hat{P}_f knowing a realization of \mathcal{G}_n can here be interpreted as a classical IS estimation for a deterministic model. Hence it follows this equality:

$$\mathbb{E}_{\tilde{\mathbf{X}}} \left[\hat{P}_f | \mathcal{G}_n \right] = \mathbb{E}_{\tilde{\mathbf{X}}} \left[\frac{1}{n_{IS}} \sum_{i=1}^{n_{IS}} w_i \mathbb{1}_{\mathcal{G}_n(\mathbf{X}_i) \leq 0}(\mathbf{X}_i) | \mathcal{G}_n \right] \quad (41)$$

$$= P_f(\mathcal{G}_n) \quad (42)$$

The probability of failure $P_f(\mathcal{G}_n)$ is here approached by an estimation by IS

$$\hat{P}_f^{IS}(\mathcal{G}_n) = \frac{1}{n_{IS}} \sum_{i=1}^{n_{IS}} w_i \mathbb{1}_{\mathcal{G}_n(\mathbf{X}_i) \leq 0}(\mathbf{X}_i),$$

with $(X_i)_{i=1, \dots, n_{IS}}$ the samples of the IS population realization. Hence, as for MCS $V_{\mathcal{G}_n}$ can be numerically obtained by computing the IS estimator of P_f for different trajectories of \mathcal{G}_n . The expression of the $V_{\mathcal{G}_n}$ estimator given by Eq. (22) for MCS becomes:

$$\widehat{V}_{\mathcal{G}_n} = \frac{1}{n_t - 1} \sum_{i=1}^{n_t} \left(\hat{P}_f^{IS}(G_i) - \frac{1}{n_t} \sum_{j=1}^{n_t} \hat{P}_f^{IS}(G_j) \right)^2 \quad (43)$$

465 where n_t is the number of \mathcal{G}_n realizations.

We can compute n_t values \hat{P}_f for n_t realizations $(G_i, \tilde{\mathbf{X}}_i)$, $i = 1, \dots, n_t$ of \mathcal{G}_n and IS population $\tilde{\mathbf{X}}$. The probability of failure can be estimated with \hat{P}_f^t as the mean of these n_t values \hat{P}_f and the total variance can be estimated using the estimator given by Eq. (24).

470 Then the estimated total COV of an estimation \hat{P}_f^{IS} of the probability of failure \hat{P}_f obtained on an IS realization is given by Eq. (27).

5.3. Extended method to Importance Sampling

In order to address low probability of failure estimation problems, we propose to integrate IS to Vb-AGP. The main idea is to replace the Monte Carlo
 475 population by an IS population for the probability of failure estimation. Thus, the variances $V_{\tilde{\mathbf{X}}}$ and $V_{\mathcal{G}_n}$ are obviously computed on the samples $\tilde{\mathbf{X}}$ generated by IS only and their estimations are obtained by applying Eq. (40) and Eq. (43). However, the learning point candidates for GP improvement correspond to all samples generated throughout the run of the NAIS algorithm \mathbf{X}^{aux} for the
 480 current auxiliary density function construction.

At the beginning of the algorithm, the initial learning point candidates are simply the samples of a classic Monte Carlo population generated with the distribution $f_{\mathbf{X}}$. Hence, the first probability of failure estimation is obtained using the MC estimator. Naturally, as soon as an IS population is used instead of the MC, the probability of failure estimator \hat{P}_f is replaced by the one corresponding to IS given by Eq. (38).

Then, steps 8 and 9 described in Sec. 4 for MCS are thus modified accordingly:

8. If $\widehat{V}_{\mathcal{G}_n} < \widehat{V}_{\mathbf{X}}$ then:

8.1. If it is the first time the algorithm passes through this loop or when \mathcal{G}_n has been updated, then a new auxiliary density function f_{aux} is built with the GP \mathcal{G}_n . IS population and candidate samples for the learning \mathbf{X}^{aux} are also replaced by the most recent ones generated. Then the algorithm goes back to step 4.

Otherwise the algorithm goes to step 8.2.

8.2. New samples are added to the IS population and the method goes back to step 4.

Else if $\widehat{V}_{\mathcal{G}_n} > \widehat{V}_{\mathbf{X}}$, the algorithm goes to step 9.

9. The learning function $EFF(\mathbf{x})$ is evaluated on the whole candidate samples population \mathbf{X}^{aux} to find the best candidate x^* to evaluate for enriching the GP metamodel. The performance function is evaluated on the sample x^* and the DoE is enriched with this new observation. Then the method goes to step 3 to update the GP model.

The extended method procedure is summarized in Fig. 8.

Moreover, as the extended method with IS may address low probability problems, there are great chances that the probability estimated with the initial DoE and MC population is equal to zero. In order to address this problem, NAIS is run one time on the GP built with the initial DoE. That allows to estimate

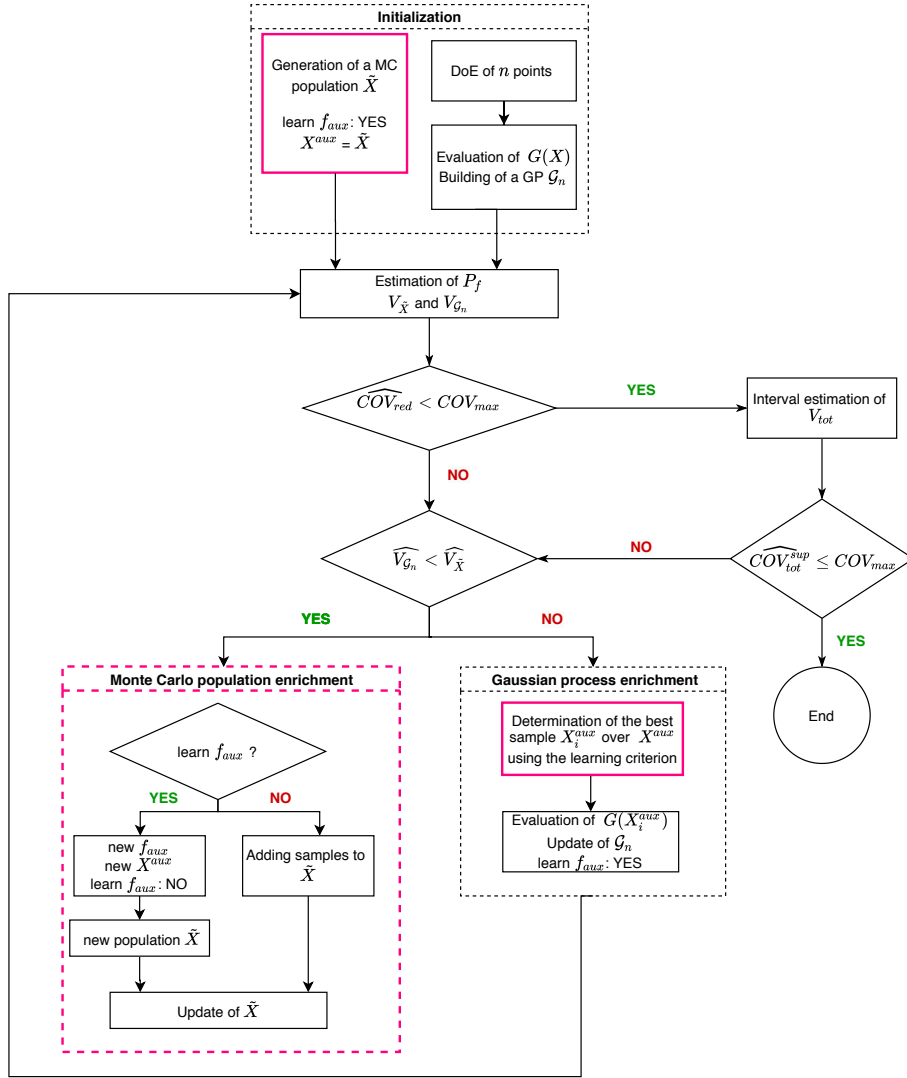


Figure 8: Flowchart of the learning algorithm improved with IS

a first auxiliary density function but also more appropriate candidate samples
 510 for the GP learning.

Indeed, for very low probability of failure, a suited initial DoE to have an appropriate initial GP approximation to allow the learning should be sampled in a certain vicinity of the limit state. However, due to the lack of information

on the failure domain at the algorithm initialisation the first estimated auxiliary
 515 density function for IS may not actually correspond to the optimal one. There-
 fore, a second initial DoE of size $2m$ more relevant for the learning is generated
 after the run of NAIS. The points of the DoE are chosen by an iterative selec-
 tion by using the *EFF* learning criterion on all intermediate samples generated
 throughout the NAIS run, with an update of the GP after each point added to
 520 the DoE.

5.4. Applications

5.4.1. Low probability series system with four branches limit state

The Vb-AGP + IS method was applied on a test case derived from the
 series system with four branches limit state function $G(\mathbf{x})$ defined by Eq. (29).
 525 The failure is defined here by $G(\mathbf{x}) \leq 1.5$ and the related reliability problem
 corresponds to a probability of failure of 5.29×10^{-5} with a COV 2.1% estimated
 by MCS (100 runs for $n_{MC} = 5 \times 10^7$). The proposed variance based method Vb-
 AGP with the adaptive IS method NAIS applied on this test case is illustrated
 on Fig. 9. On this Figure, the intermediate population used as GP learning
 530 samples and the IS population used to compute the probability are represented.

The mean results over 100 runs of the algorithm on this test case are given
 in Tab. 4. They show that the Vb-AGP + IS method allows to respect the
 maximal COV set to 3% on the 100 runs of the algorithm.

Method	N_{call}	$COV(N_{call})$	\hat{P}_f	$COV(\hat{P}_f)$	e_r	ν_{MC}
MCS	5×10^7	-	5.29×10^{-5}	2.1%	-	-
Vb-AGP + IS	104	16.2%	5.33×10^{-5}	3.0%	2.4%	201437

Table 4: Series system with four branches low probability of failure problem - 100 run mean
 results - Adaptive method parameters: $n_{DoE}^{init} = 12$, $COV_{max} = 0.03$.

Here, we do not compare the method to AK-MCS because this type of
 535 reliability problem with low probabilities of failure is difficult to address with

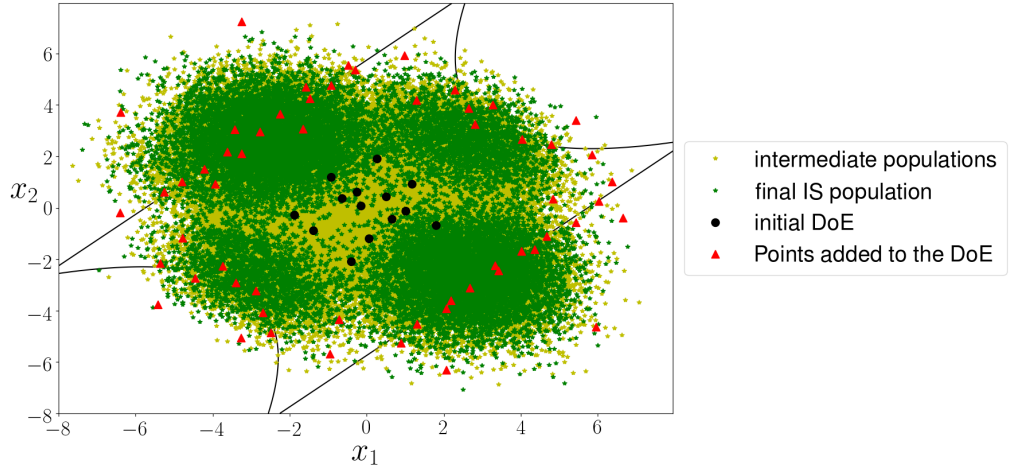


Figure 9: Vb-AGP + IS (NAIS) method

this method and neither to AK-IS [5] as the method is based on FORM and thus not suited for multimodal failure domains. Nonetheless, it can be noted that the efficiency indicator ν_{MC} of the method in comparison to MCS is very high.

540 *5.4.2. Dynamic response of an oscillator*

The variance based GP+IS method was then applied on the second case derived from the example dealing with the dynamic response of an oscillator with a non-linear limit state function, described in Sec. 4.3.3, with $F_1 \sim \mathcal{N}(0.6, 0.01)$ corresponding to an estimated probability of failure of 9.08×10^{-6} ($COV =$
 545 2.47%) with MCS. The method was run 50 times for initial DoEs of 12 samples and a maximum coefficient of variation of 3%.

Obviously, this reliability problem is intractable with the AK-MCS method but has been handled by the method AK-IS [5]. Hence, we compare the mean results of the Vb-AGP + IS approach with the results of AK-IS presented in
 550 the paper [5]. These results are given in Tab. 5.

On this example, the method Vb-AGP divides on average the number of calls

Method	N_{call}	$COV(N_{call})$	\hat{P}_f	$COV(\hat{P}_f)$	e_r	ν_{MC}
MCS	1.8×10^9	-	9.08×10^{-6}	2.47%	-	-
FORM+ IS	$29 + 10^4$	-	9.13×10^{-6}	2.29%	-	-
AK-IS [5]	$29 + 38$	-	9.13×10^{-6}	2.29%	-	1943812
Vb-AGP + IS	58	20%	9.09×10^{-6}	2.9%	2.3%	2240946

Table 5: Result for the oscillator test case ($\mu_{F_1} = 0.6, \sigma_{F_1} = 0.1$) — 100 run mean results
Adaptive method parameters: $n_{DoE}^{init} = 12, COV_{max} = 0.03$.

to the performance function by AK-IS by a factor 1.16. This reduction is less important than the ones obtained on the previous examples with AK-MCS. Note that the COV of N_{call} is relatively high for the method Vb-AGP+IS. That can
555 be explained by the influence of the initial DoE, that has an important impact on the performances of NAIS. Moreover, six random variables are considered on this example and thus the efficiency of NAIS is considerably reduced as the stochastic dimension is quite high for the applicability of this method.

5.4.3. Reliability analysis on a thermal problem

560 5.4.3.1. Description of the problem

. In this section, the proposed method is applied to a finite element based reliability analysis, involving the heat transfer through the combustion chamber wall of a regeneratively cooled rocket engine [47, 48, 49]. In such an engine, liquid hydrogen (LH2) flowing through cooling channels in the combustion chamber
565 wall at a temperature of 40K is used for cooling the engine. We consider that failure occurs when the maximum temperature of the inner wall of the combustion chamber exceeds a critical value T_{allow} , which corresponds to the cooling channel walls rupture, due to thermally induced stresses.

A schematic of the combustion chamber of a typical regeneratively cooled
570 liquid hydrogen (LH2) liquid oxygen (LOX) rocket engine is shown in Fig. 10. As illustrated, two different parts made of two different materials form the com-

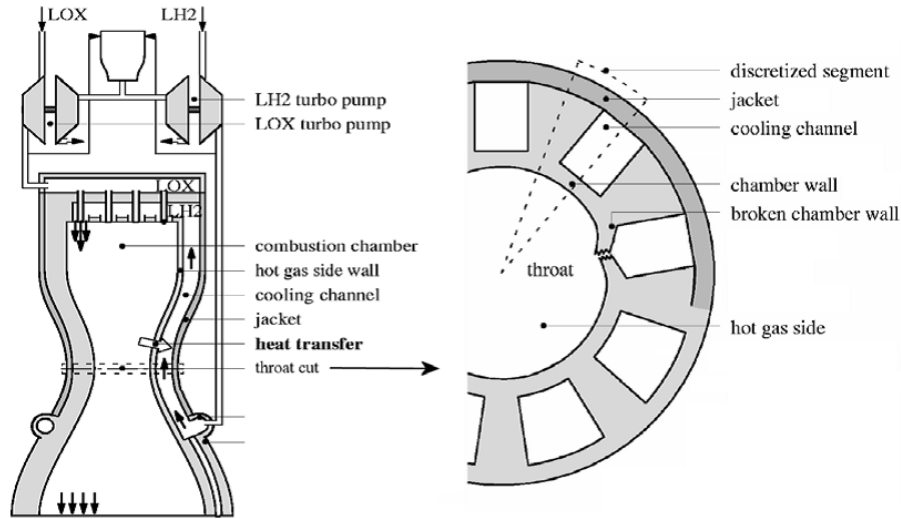


Figure 10: Schematic of a regeneratively cooled rocket engine combustion chamber.

bustion chamber wall: an internal side made of a copper alloy and an external
 jacket made of a Ni alloy. Heat exchanges may happen through convection be-
 tween the combustion chamber wall and the sources of heat (combustion cham-
 ber gases) and cooling (liquid hydrogen) and also with the exterior. Considering
 575 these boundary conditions, the resulting thermal transfer depends on the fol-
 lowing parameters: the conductivity of the inner side of the wall (k_{Cu}), the
 conductivity of the jacket (k_{Ni}), the temperature of the gases on the inner side
 of the combustion chamber (T_{hot}), the film convection coefficient on the inner
 580 side of the combustion chamber (h_{hot}), the temperature on the outer side of the
 combustion chamber (T_{out}), the film convection coefficient on the outer side of
 the combustion chamber (h_{out}), the temperature of the cooling fluid (T_{cool}) and
 the film convection coefficient on the cooling channel side (h_{cool}).

Here the thermal field is computed using an in-house finite element solver
 585 coded in Python. Thus we have access to the maximum temperature in order to
 deduce the value of the performance function, defined here as $G(\mathbf{x}) = T_{allow}(\mathbf{x}) - T_{max}(\mathbf{x})$.
 Then the failure probability can be estimated using sampling methods or en-
 hanced methods such as active learning strategies.

A reliability-based sensitivity analysis was carried out on this problem and
 590 the parameters h_{out} and k_{Cu} were shown to have negligible influence on the
 failure. Other parameters and the maximum temperature allowable T_{allow} are
 supposed to be uncertain and are modeled by independent random variables
 following probability distributions given in Table 6. The thermal field at sta-
 tionary equilibrium is obtained by resolution of a convection-diffusion equation
 595 by a finite element approach. The finite element mesh of the combustion
 chamber wall and the boundary conditions are illustrated in Fig. 11.

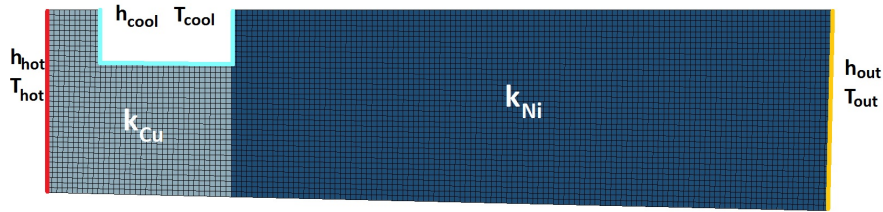


Figure 11: Finite element mesh of the combustion chamber wall and the boundary conditions of the thermal problem.

Input	k_{Ni}	T_{hot}	h_{hot}	T_{out}	T_{cool}	h_{cool}	T_{allow}
Unit	W/mK	K	kW/m^2K	K	K	kW/m^2K	K
Probability law	Gaussian	Uniform	Uniform	Uniform	Uniform	Uniform	Uniform
Mean	75	880	31	293	40	250	730
<i>COV</i>	2%	-	-	-	-	-	-
Half-range	-	10%	10%	5%	5%	10%	7.5%

Table 6: Probability distributions of the thermal problem parameters.

5.4.3.2. Results

. As this example involved a costly numerical resolution only the Ak-MCS + U and the proposed Vb-AGP + IS methods are compared. For both approaches
 600 the targeted maximum coefficient of variation is set to 3% and the initial DoEs count 10 samples. In order to assess the robustness of the approaches, 50 runs on different initial DoEs are performed. The results are given in the table 7.

Method	N_{call}	$COV(N_{call})$	\hat{P}_f	$COV(\hat{P}_f)$	$\nu_{MC}^{N_{call}}$
AK-MCS + U	30.36	6.61%	7.15×10^{-4}	3.21%	44707
Vb-AGP + IS	15.04	1.30%	7.04×10^{-4}	3.12%	97022

Table 7: Result for the combustion chamber test case — 50 run mean results
 Adaptive method parameters: $n_{DoE}^{init} = 10$, $COV_{max} = 0.03$.

These results show that the two methods converge to the same probability of failure estimation which allows to be confident in this estimation. Moreover, for
 605 both approaches, this estimation is reached with a coefficient of variation close to 3%. It is recall that, for the proposed Vb-AGP + IS approach, this coefficient of variation takes into account the uncertainty due to the IS and the uncertainty due to the use of the GP surrogate model. This example hence confirms that the estimator of the total coefficient of variation proposed in Section 5.1 can be
 610 trusted. Finally it is notable that the proposed Vb-AGP + IS method needs on this problem about two times less calls to the performance function than the AK-MCS + U method (the numerical efficiency metric $\nu_{MC}^{N_{call}}$ is about two times larger for Vb-AGP + IS than for AK-MCS + U).

6. Conclusions

615 In this paper, we showed that the effect of both the Monte Carlo sampling and the GP surrogate model on the probability of failure estimator can be analyzed by a sensitivity analysis based on variance decomposition. Then we have

proposed estimators of the variances related to each of these two uncertainty sources and also an estimator of the total variance in order to compute them numerically. This analysis enables us to quantify the source of uncertainty that has the most impact on the variability of the probability of failure estimation.

Then we proposed a Variance based Active GP (Vb-AGP) learning procedure that integrates this analysis to improve the major source of uncertainty during the learning phase and a stopping criterion based on the total variance of the probability of failure estimation. The method was applied to two examples and showed great potential to reduce the number of learning points while satisfying the maximum COV constraint imposed by the user. Moreover, the method gives an estimation of the total COV that has been validated on the various examples.

An extension of this method to IS, in order to make it more suitable to probability of rare events estimation, was then presented. In this work, the adaptive IS algorithm NAIS was used in order to tackle multimodal failure domains without any a priori knowledge of the domain. The approach was applied to three examples and was shown effective in terms of the accuracy of the probability of failure total COV estimations and also in terms of potential number of simulations reduction. However, it should be noted that the application of Vb-AGP + MCS is limited to problems with a relatively low stochastic dimension because of the memory cost of accurate trajectory simulations with the Karhunen-Loeve expansion for large MC populations. Hence, a potential improvement of the method could be thought by looking to improve the efficiency of the trajectory simulations technique while taking care that the trajectories approximations are sufficiently accurate.

Note also that the use of the Vb-AGP + IS method is a good way to reduce the sampling population size, but as the NAIS algorithm is only efficient for problems with relatively low input dimensionality ($m < 10$) it is also not suited for problems with high stochastic dimensions. In this work, an extension to rare events problems with NAIS was chosen as we considered that there is no a priori knowledge of the limit state. However, in case some hypothesis about the limit state form are available by experience for example, other IS or Subset Sampling

techniques might be considered to circumvent the curse of dimensionality.

650 **Acknowledgment**

This work was supported by the French National Research Agency (ANR) through the ReBRReD project under grant ANR-16-CE10-0002.

Appendix A. Gaussian process trajectories computations by simulating an unconditioned Gaussian process

655 The objective here is to explain how to avoid numerical issues experienced when simulating GP trajectories with large population.

We saw in Sec. 3.2 that the estimation of $V_{\mathcal{G}_n}$ can be assessed from realizations of the Gaussian process \mathcal{G}_n at each point of the sampled population.

Let \mathcal{G}_n be a conditioned GP with mean function $\boldsymbol{\mu}_n(\cdot)$ and covariance matrix $\mathbf{C}_n(\cdot)$. A trajectory (or realization) of the GP \mathcal{G}_n at the Monte Carlo population $\tilde{\mathbf{X}}$ can actually be expressed as follows:

$$\mathcal{G}_n(\tilde{\mathbf{X}}) = \boldsymbol{\mu}_n(\tilde{\mathbf{X}}) + \mathbf{L}_n(\tilde{\mathbf{X}})\boldsymbol{\xi} \tag{A.1}$$

with $\boldsymbol{\xi} \sim \mathcal{N}(\mathbf{0}_n, \mathbf{I}_n)$ and $\mathbf{L}_n(\tilde{\mathbf{X}}) \in M^{n_{MC}}(\mathbb{R})$ the Cholesky factorization matrix of $\mathbf{C}_n(\tilde{\mathbf{X}})$, i.e. $\mathbf{C}_n(\tilde{\mathbf{X}}) = \mathbf{L}_n(\tilde{\mathbf{X}})\mathbf{L}_n(\tilde{\mathbf{X}})^T$.
660

However for large populations, the computation of $\mathcal{G}_n(\tilde{\mathbf{X}})$ realizations present huge numerical costs or encounter numerical issues like ill-conditioned covariance matrix, making it impossible to compute the Cholesky decomposition and thus the GP realizations by this method. These numerical problems can be avoided by simulating an unconditioned Gaussian process [15, 37, 33].
665

Let $\tilde{\mathcal{G}}(\mathbf{x})$ be a centered Gaussian process with the same covariance function as $\mathcal{G}(\mathbf{x})$:

$$\tilde{\mathcal{G}}(\mathbf{x}) \sim GP(0, \sigma_Z^2 r(\mathbf{x}, \mathbf{x}')) \tag{A.2}$$

and let $\tilde{\boldsymbol{\mu}}(\mathbf{x})$ be its prediction mean based on the random variables $\tilde{\mathcal{G}}(\mathbf{x}_{doe})$.

Then, let us define the Gaussian process $\tilde{\mathcal{G}}_n(\mathbf{x})$:

$$\tilde{\mathcal{G}}_n(\mathbf{x}) = \boldsymbol{\mu}_n(\mathbf{x}) - \tilde{\boldsymbol{\mu}}(\mathbf{x}) + \tilde{\mathcal{G}}(\mathbf{x}) \tag{A.3}$$

with $\mu_n(\mathbf{x})$ the mean of the prediction by $\mathcal{G}_n(\mathbf{x})$ at point \mathbf{x} and:

$$\tilde{\mu}(\mathbf{x}) = \mathbf{f}(\mathbf{x})^T \tilde{\boldsymbol{\beta}} + \mathbf{k}(\mathbf{x})^T \mathbf{C}^{-1}(\mathbf{y} - \mathbf{F}\tilde{\boldsymbol{\beta}}) \quad (\text{A.4})$$

with $\tilde{\boldsymbol{\beta}} = (\mathbf{F}^T \mathbf{C}^{-1} \mathbf{F})^{-1} \mathbf{F}^T \mathbf{C}^{-1} \tilde{\mathcal{G}}(\mathbf{x}_{doe})$.

Then, $\tilde{\mathcal{G}}_n(\mathbf{x})$ has the same distribution as $\mathcal{G}_n(\mathbf{x})$ conditionally to past observations $(\mathbf{x}_{doe}, \mathbf{y})$. In other words, we have:

$$\tilde{\mathcal{G}}_n(\mathbf{x}) \stackrel{\mathcal{L}}{=} \mathcal{G}_n(\mathbf{x}) \quad (\text{A.5})$$

Hence, a simulation of $\mathcal{G}_n(\mathbf{x})$ can be obtained by adding to its mean $\mu_n(\mathbf{x})$ the prediction error $\tilde{\mathcal{G}}(\mathbf{x}) - \tilde{\mu}(\mathbf{x})$ of $\tilde{\mathcal{G}}(\mathbf{x})$. It allows to simulate the centered
 670 Gaussian process $\tilde{\mathcal{G}}(\mathbf{x})$ instead of $\mathcal{G}_n(\mathbf{x})$. Contrary to the conditioned Gaussian process, the unconditioned Gaussian process variance values at points in the vicinity of the DOE are not close to zero. It allows a better conditioning of the covariance matrix and thus avoids the related numerical issues.

Moreover, it allows to use computationally efficient representations of random
 675 fields such as the Karhunen-Loève (KL) expansion. The numerical approximation of the KL expansion can be obtained by using the Nyström procedure or Galerkin methods as presented in [50]. Hence, once the KL decomposition of the Gaussian process $\tilde{\mathcal{G}}(\mathbf{x})$ is estimated it can be used to easily obtain realizations at any point \mathbf{x} using Eq. (A.3).

680 Appendix B. Non parametric adaptive importance sampling (NAIS)

The goal of the non parametric adaptive importance sampling (NAIS) algorithm is to compute an estimator of the optimal auxiliary density function f_{aux}^{opt} , given by Eq. (37), with standard Gaussian kernel density functions $K_d(\cdot)$ weighted with weights w , starting from the input density function $f_{\mathbf{X}}$. This
 685 method is well adapted to complex failure region D_f .

The different steps of the algorithm are described in Algorithm 2.

The successive NAIS iterations allow to update the estimator of the optimal auxiliary density function \hat{g}_{opt}^k . In the end we obtain the estimator of the optimal

690 auxiliary density function of the initial sought probability $P_f = \mathbb{P}[\mathcal{G}_n(\mathbf{X}) \leq 0]$.
 The probability is then estimated with the IS formula (line 19 Algorithm 2).

Algorithm 2 Non parametric Adaptive Importance Sampling (NAIS)

Require: $\rho, n_{IS}, f_{\mathbf{X}}, \mathcal{G}_n$

- 1: $k \leftarrow 0$
 - 2: $\tilde{\mathbf{X}}^0 \leftarrow$ population generated from $f_{\mathbf{X}}$ of cardinal n_{IS}
 - 3: $\mathbf{Y}^0 \leftarrow \mathcal{G}_n(\tilde{\mathbf{X}}^0)$
 - 4: $S^* \leftarrow \rho$ -quantile of \mathbf{Y}^0
 - 5: $\gamma_0 \leftarrow \max(S^*, 0)$
 - 6: $\mathbf{w}^0 \leftarrow \mathbb{1}_{\mathbf{Y}^0 \leq \gamma_0}$
 - 7: $I_0 \leftarrow \frac{1}{n_{IS}} \sum_{i=1}^{n_{IS}} w_i^0$
 - 8: $\hat{g}_{opt}^1(\mathbf{x}) \leftarrow \frac{1}{n_{IS} \det(B_N) I_0} \sum_{i=1}^{n_{IS}} w_i^0 K_d(B_N^{-1}(\mathbf{x} - \mathbf{X}_i^0))$
 - 9: **while** $\gamma_k > 0$ **do**
 - 10: $k \leftarrow k + 1$
 - 11: $\tilde{\mathbf{X}}^k \leftarrow$ population generated from \hat{g}_{opt}^k of cardinal n_{IS}
 - 12: $\mathbf{Y}^k \leftarrow \mathcal{G}_n(\tilde{\mathbf{X}}^k)$
 - 13: $S^* \leftarrow \rho$ -quantile of \mathbf{Y}^k
 - 14: $\gamma_k \leftarrow \max(S^*, 0)$
 - 15: $w_i^j \leftarrow \frac{\mathbb{1}_{\mathbf{Y}_i^j \leq \gamma_k} f_{\mathbf{X}}(\mathbf{X}_i^j)}{\hat{g}_{opt}^j(\mathbf{X}_i^j)}$, for $i, j \in [1, n_{IS}] \times [1, k]$
 - 16: $I_k \leftarrow \frac{1}{kn_{IS}} \sum_{j=1}^k \sum_{i=1}^{n_{IS}} w_i^j$
 - 17: $\hat{g}_{opt}^{k+1}(\mathbf{x}) \leftarrow \frac{1}{kn_{IS} \det(B_N) I_k} \sum_{j=1}^k \sum_{i=1}^{n_{IS}} w_i^j K_d(B_N^{-1}(\mathbf{x} - \mathbf{X}_i^j))$
 - 18: **end while**
 - 19: $\hat{P}_f^{NAIS} \leftarrow \frac{1}{n_{IS}} \sum_{i=1}^{n_{IS}} \frac{\mathbb{1}_{\mathbf{Y}^k \leq 0} f_{\mathbf{X}}(\mathbf{X}_i^k)}{\hat{g}_{opt}^k(\mathbf{X}_i^k)}$
-

In Algorithm 2 line 8, B_N is a diagonal covariance matrix.

In practice the GP prediction mean is used to evaluate the samples. However in the proposed method, the NAIS algorithm is used in intermediate steps were the GP approximation of the limit state may not be accurate. Hence, it is more appropriate to use an auxiliary density suited to estimate the probability $\hat{P}_f^{NAIS} = \frac{1}{n_{IS}} \sum_{i=1}^{n_{IS}} p(\mathbf{X}_i) \frac{f_{\mathbf{X}}(\mathbf{X}_i)}{\hat{g}_{opt}^k(\mathbf{X}_i)}$. Therefore in our method, the NAIS

algorithm is run with weights computed as follows:

$$w_i^j = \frac{\mathbb{P}[\mathcal{G}_n(\mathbf{X}_i^j) \leq \gamma_k] f_{\mathbf{X}}(\mathbf{X}_i^j)}{\hat{g}_{opt}^j(\mathbf{X}_i^j)}, \quad \text{for } i, j \in [1, n_{IS}] \times [1, k] \quad (\text{B.1})$$

with $\mathbb{P}[\mathcal{G}_n(\mathbf{X}) \leq \gamma_k] = \Phi\left(\frac{\gamma_k - \mu_n(\mathbf{x})}{\sigma_n(\mathbf{x})}\right)$

Moreover, in case of very low probability of failure the run of NAIS with the first built GPs can fail as the mean predicted values become quasi constant as
 695 the NAIS intermediate populations expand outward the known points. This is due to the initial large uncertainty on the failure domain. Therefore, a maximum relative residual between two consecutive intermediate thresholds γ_k must be set. On our test cases, a relative residual of 10^{-3} has been set.

References

- 700 [1] M. Lemaire, Structural reliability, ISTE, Wiley, Hoboken, NJ, 2010 (2010).
 URL <https://cds.cern.ch/record/1608589>
- [2] R. E. Melchers, A. T. Beck, Structural Reliability Analysis and Prediction, John Wiley & Sons, 2018, google-Books-ID: 8yE6DwAAQBAJ (Apr. 2018).
- [3] C. Bucher, T. Most, A comparison of approximate response functions
 705 in structural reliability analysis, Probabilistic Engineering Mechanics 23 (2008) 154–163 (04 2008). doi:10.1016/j.probengmech.2007.12.022.
- [4] E. Vazquez, J. Bect, A sequential Bayesian algorithm to estimate a probability of failure, IFAC Proceedings Volumes 42 (10) (2009) 546–550 (Jan. 2009). doi:10.3182/20090706-3-FR-2004.00090.
 710 URL <http://www.sciencedirect.com/science/article/pii/S1474667016387043>
- [5] B. Echard, N. Gayton, M. Lemaire, N. Relun, A combined Importance Sampling and Kriging reliability method for small failure probabilities with time-demanding numerical models, Reliability Engineering & System Safety 111 (Supplement C) (2013) 232–240 (Mar. 2013).
 715

doi:10.1016/j.ress.2012.10.008.

URL <http://www.sciencedirect.com/science/article/pii/S0951832012002086>

- 720 [6] B. J. Bichon, M. S. Eldred, L. P. Swiler, S. Mahadevan, J. M. McFarland,
Efficient Global Reliability Analysis for Nonlinear Implicit Performance
Functions, *AIAA Journal* 46 (10) (2008) 2459–2468 (Oct. 2008). doi:
10.2514/1.34321.

URL <http://arc.aiaa.org/doi/10.2514/1.34321>

- 725 [7] B. J. Bichon, J. M. McFarland, S. Mahadevan, Efficient surrogate models
for reliability analysis of systems with multiple failure modes, *Reliability
Engineering & System Safety* 96 (10) (2011) 1386–1395 (Oct. 2011).
doi:10.1016/j.ress.2011.05.008.

URL <http://www.sciencedirect.com/science/article/pii/S0951832011001062>

- 730 [8] W. Fauriat, N. Gayton, AK-SYS: An adaptation of the AK-MCS method
for system reliability, *Reliability Engineering & System Safety* 123 (2014)
137–144 (Mar. 2014). doi:10.1016/j.ress.2013.10.010.

URL <http://www.sciencedirect.com/science/article/pii/S0951832013002949>

- 735 [9] L. Li, J. Bect, E. Vazquez, Bayesian Subset Simulation: a kriging-based
subset simulation algorithm for the estimation of small probabilities of fail-
ure, in: 11th International Probabilistic Assessment and Management Con-
ference (PSAM11) and The Annual European Safety and Reliability Con-
ference (ESREL 2012), Helsinki, Finland, 2012, pp. CD-ROM Proceedings
740 (10 pages) (Jun. 2012).

URL <https://hal-supelec.archives-ouvertes.fr/hal-00715316>

- [10] J. Bect, D. Ginsbourger, L. Li, V. Picheny, E. Vazquez, Sequential
design of computer experiments for the estimation of a probability of
failure, *Statistics and Computing* 22 (3) (2012) 773–793 (May 2012).

- 745 doi:10.1007/s11222-011-9241-4.
URL <https://link.springer.com/article/10.1007/s11222-011-9241-4>
- [11] V. Dubourg, B. Sudret, F. Deheeger, Metamodel-based importance sampling for structural reliability analysis, *Probabilistic Engineering Mechanics* 33 (2013) 47–57 (Jul. 2013). doi:10.1016/j.probengmech.2013.02.002.
750 URL <http://www.sciencedirect.com/science/article/pii/S0266892013000222>
- [12] A. Basudhar, S. Missoum, Reliability assessment using probabilistic support vector machines, *International Journal of Reliability and Safety* 7 (2) (2013) 156–173 (Jan. 2013). doi:10.1504/IJRS.2013.056378.
755 URL <https://www.inderscienceonline.com/doi/abs/10.1504/IJRS.2013.056378>
- [13] J. M. Bourinet, F. Deheeger, M. Lemaire, Assessing small failure probabilities by combined subset simulation and Support Vector
760 Machines, *Structural Safety* 33 (6) (2011) 343–353 (Sep. 2011). doi:10.1016/j.strusafe.2011.06.001.
URL <http://www.sciencedirect.com/science/article/pii/S0167473011000555>
- [14] Schöbi R., Sudret B., Marelli S., Rare Event Estimation Using Polynomial-
765 Chaos Kriging, *ASCE-ASME Journal of Risk and Uncertainty in Engineering Systems, Part A: Civil Engineering* 3 (2) (2017) D4016002 (Jun. 2017). doi:10.1061/AJRUA6.0000870.
URL <https://ascelibrary.org/doi/abs/10.1061/AJRUA6.0000870>
- [15] C. E. Rasmussen, C. K. I. Williams, Gaussian processes for machine learning, Adaptive computation and machine learning, MIT Press, Cambridge,
770 Mass, 2006, oCLC: ocm61285753 (2006).
- [16] A. I. Forrester, A. J. Keane, Recent advances in surrogate-based optimization, *Progress in Aerospace Sciences* 45 (1-3) (2009) 50–79 (Jan. 2009).

doi:10.1016/j.paerosci.2008.11.001.

775 URL <http://linkinghub.elsevier.com/retrieve/pii/S0376042108000766>

[17] B. Echard, N. Gayton, M. Lemaire, AK-MCS: An active learning reliability method combining Kriging and Monte Carlo Simulation, *Structural Safety* 33 (2) (2011) 145–154 (Mar. 2011).
780 doi:10.1016/j.strusafe.2011.01.002.

URL <http://www.sciencedirect.com/science/article/pii/S0167473011000038>

[18] X. Huang, J. Chen, H. Zhu, Assessing small failure probabilities by AK-SS: An active learning method combining Kriging and Subset Simulation, *Structural Safety* 59 (Supplement C) (2016) 86–95 (Mar. 2016).
785 doi:10.1016/j.strusafe.2015.12.003.

URL <http://www.sciencedirect.com/science/article/pii/S0167473016000035>

[19] N. Lelièvre, P. Beaurepaire, C. Mattrand, N. Gayton, AK-MCSi: A
790 Kriging-based method to deal with small failure probabilities and time-consuming models, *Structural Safety* 73 (2018) 1–11 (Jul. 2018).
doi:10.1016/j.strusafe.2018.01.002.

URL <http://www.sciencedirect.com/science/article/pii/S0167473017301558>

795 [20] M. Balesdent, J. Morio, J. Marzat, Kriging-based adaptive Importance Sampling algorithms for rare event estimation, *Structural Safety* 44 (Supplement C) (2013) 1–10 (Sep. 2013). doi:10.1016/j.strusafe.2013.04.001.

800 URL <http://www.sciencedirect.com/science/article/pii/S0167473013000350>

[21] F. Cadini, A. Gioletta, A Bayesian Monte Carlo-based algorithm for the estimation of small failure probabilities of systems affected by uncer-

tainties, Reliability Engineering & System Safety 153 (2016) 15–27 (Sep. 2016). doi:10.1016/j.ress.2016.04.003.

805 URL <http://www.sciencedirect.com/science/article/pii/S0951832016300175>

[22] F. Cadini, F. Santos, E. Zio, An improved adaptive kriging-based importance technique for sampling multiple failure regions of low probability, Reliability Engineering & System Safety 131 (2014) 109–117 (Nov. 2014).
810 doi:10.1016/j.ress.2014.06.023.

URL <http://linkinghub.elsevier.com/retrieve/pii/S0951832014001537>

[23] Z. Lv, Z. Lu, P. Wang, A new learning function for Kriging and its applications to solve reliability problems in engineering, Computers & Mathematics with Applications 70 (5) (2015) 1182–1197 (Sep. 2015).
815 doi:10.1016/j.camwa.2015.07.004.

URL <http://www.sciencedirect.com/science/article/pii/S0898122115003399>

[24] X. Zhang, L. Wang, J. D. Sørensen, REIF: A novel active-learning function toward adaptive Kriging surrogate models for structural reliability
820 analysis, Reliability Engineering & System Safety 185 (2019) 440–454 (May 2019). doi:10.1016/j.ress.2019.01.014.

URL <http://www.sciencedirect.com/science/article/pii/S0951832018305969>

825 [25] Z. Wang, A. Shafieezadeh, REAK: Reliability analysis through Error rate-based Adaptive Kriging, Reliability Engineering & System Safety 182 (2019) 33–45 (Feb. 2019). doi:10.1016/j.ress.2018.10.004.

URL <http://www.sciencedirect.com/science/article/pii/S0951832017312504>

830 [26] B. Gaspar, A. P. Teixeira, C. Guedes Soares, Adaptive surrogate model with active refinement combining Kriging and a trust region method,

Reliability Engineering & System Safety 165 (2017) 277–291 (Sep. 2017).
doi:10.1016/j.ress.2017.03.035.

URL <http://www.sciencedirect.com/science/article/pii/S0951832016301892>

835

- [27] G. Perrin, Active learning surrogate models for the conception of systems with multiple failure modes, Reliability Engineering & System Safety 149 (2016) 130–136 (May 2016). doi:10.1016/j.ress.2015.12.017.

URL <http://www.sciencedirect.com/science/article/pii/S0951832015003695>

840

- [28] Z. Wang, A. Shafieezadeh, ESC: an efficient error-based stopping criterion for kriging-based reliability analysis methods, Structural and Multidisciplinary Optimization 59 (5) (2019) 1621–1637 (May 2019). doi:10.1007/s00158-018-2150-9.

URL <https://doi.org/10.1007/s00158-018-2150-9>

845

- [29] J. Morio, M. Balesdent, D. Jacquemart, C. Vergé, A survey of rare event simulation methods for static input–output models, Simulation Modelling Practice and Theory 49 (2014) 287–304 (2014).

- [30] D. G. Krige, A statistical approach to some basic mine valuation problems on the Witwatersrand, Journal of the Southern African Institute of Mining and Metallurgy 52 (6) (1951) 119–139 (Dec. 1951).

850

URL https://journals.co.za/content/saimm/52/6/AJA0038223X_4792

- [31] G. Matheron, Principles of geostatistics, Economic Geology 58 (8) (1963) 1246–1266 (Dec. 1963). doi:10.2113/gsecongeo.58.8.1246.

855

URL <https://pubs.geoscienceworld.org/segweb/economicgeology/article-abstract/58/8/1246/17275/principles-of-geostatistics>

- [32] D. R. Jones, A Taxonomy of Global Optimization Methods Based on Response Surfaces, Journal of Global Optimization 21 (4) (2001) 345–383

- 860 (Dec. 2001). doi:10.1023/A:1012771025575.
URL <https://doi.org/10.1023/A:1012771025575>
- [33] L. Le Gratiet, C. Cannamela, B. Iooss, A Bayesian Approach for Global Sensitivity Analysis of (Multifidelity) Computer Codes, SIAM/ASA Journal on Uncertainty Quantification 2 (1) (2014) 336–363 (Jan. 2014). doi:10.1137/130926869.
865 URL <https://epubs.siam.org/doi/abs/10.1137/130926869>
- [34] Z. Zhu, X. Du, Reliability Analysis With Monte Carlo Simulation and Dependent Kriging Predictions, Journal of Mechanical Design 138 (12) (Dec. 2016). doi:10.1115/1.4034219.
870 URL <https://asmedigitalcollection.asme.org/mechanicaldesign/article/138/12/121403/376322/Reliability-Analysis-With-Monte-Carlo-Simulation>
- [35] A.-K. El Haj, A.-H. Soubra, Improved active learning probabilistic approach for the computation of failure probability, Structural Safety 88 (2021) 102011 (Jan. 2021). doi:10.1016/j.strusafe.2020.102011.
875 URL <http://www.sciencedirect.com/science/article/pii/S0167473020300904>
- [36] B. Iooss, P. Lemaitre, A Review on Global Sensitivity Analysis Methods, in: G. Dellino, C. Meloni (Eds.), Uncertainty Management in Simulation-Optimization of Complex Systems: Algorithms and Applications, Operations Research/Computer Science Interfaces Series, Springer US, Boston, MA, 2015, pp. 101–122 (2015). doi:10.1007/978-1-4899-7547-8_5.
880 URL https://doi.org/10.1007/978-1-4899-7547-8_5
- [37] J. Villemonteix, E. Vazquez, E. Walter, An informational approach to the global optimization of expensive-to-evaluate functions, Journal of Global Optimization 44 (4) (2009) 509–534 (2009). doi:10.1007/s10898-008-9354-2.
885 URL <https://hal-supelec.archives-ouvertes.fr/hal-00354262>

- [38] G. Archer, A. Saltelli, I. Sobol, Sensitivity measures, ANOVA-like techniques and the use of bootstrap, *Journal of Statistical Computation and Simulation* 58 (2) (1997) 99–120 (1997).
890
- [39] A. Borri, E. Speranzini, Structural reliability analysis using a standard deterministic finite element code, *Structural Safety* 19 (4) (1997) 361–382 (1997).
- [40] R. Zimmermann, On the condition number anomaly of Gaussian correlation matrices, *Linear Algebra and its Applications* 466 (2015) 512–526 (Feb. 2015). doi:10.1016/j.laa.2014.10.038.
905
URL <http://www.sciencedirect.com/science/article/pii/S0024379514007174>
- [41] B. Echard, Kriging-based reliability assessment of structures submitted to fatigue, PhD Thesis, Université Blaise Pascal (2012).
900
- [42] J. Bucklew, Introduction to rare event simulation, Springer Science & Business Media, 2013 (2013).
- [43] P.-T. De Boer, D. P. Kroese, S. Mannor, R. Y. Rubinstein, A tutorial on the cross-entropy method, *Annals of operations research* 134 (1) (2005) 19–67 (2005).
905
- [44] P. Zhang, Nonparametric importance sampling, *Journal of the American Statistical Association* 91 (435) (1996) 1245–1253 (1996).
- [45] I. Papaioannou, C. Papadimitriou, D. Straub, Sequential importance sampling for structural reliability analysis, *Structural safety* 62 (2016) 66–75 (2016).
910
- [46] J. Morio, Extreme quantile estimation with nonparametric adaptive importance sampling, *Simulation Modelling Practice and Theory* 27 (2012) 76–89 (09 2012). doi:10.1016/j.simpat.2012.05.008.

- 915 [47] J. Riccius, O. Haidn, E. Zametaev, Influence of Time Dependent Effects on the Estimated Life Time of Liquid Rocket Combustion Chamber Walls, in: 40th AIAA/ASME/SAE/ASEE Joint Propulsion Conference and Exhibit, American Institute of Aeronautics and Astronautics. doi:10.2514/6.2004-3670.
- 920 URL <https://arc.aiaa.org/doi/abs/10.2514/6.2004-3670>
- [48] J. Riccius, E. Zametaev, O. Haidn, C. Gogu, LRE Chamber Wall Optimization Using Plane Strain and Generalized Plane Strain Models, in: 42nd AIAA/ASME/SAE/ASEE Joint Propulsion Conference & Exhibit, American Institute of Aeronautics and Astronautics. doi:10.2514/6.2006-4366.
- 925 URL <https://arc.aiaa.org/doi/abs/10.2514/6.2006-4366>
- [49] C. Gogu, A. Chaudhuri, C. Bes, How Adaptively Constructed Reduced Order Models Can Benefit Sampling-Based Methods for Reliability Analyses, International Journal of Reliability, Quality and Safety Engineering 23 (05) (2016) 1650019 (2016).
- 930 [50] W. Betz, I. Papaioannou, D. Straub, Numerical methods for the discretization of random fields by means of the Karhunen–Loève expansion, Computer Methods in Applied Mechanics and Engineering 271 (2014) 109–129 (Apr. 2014). doi:10.1016/j.cma.2013.12.010.
- URL <http://www.sciencedirect.com/science/article/pii/S0045782513003502>
- 935